



Calhoun: The NPS Institutional Archive

Faculty and Researcher Publications

Faculty and Researcher Publications

2013

Discretely exact derivatives for hyperbolic PDE-constrained optimization problems discretized by the discontinuous Galerkin method, Draft



Calhoun is a project of the Dudley Knox Library at NPS, furthering the precepts and goals of open government and government transparency. All information contained herein has been approved for release by the NPS Public Affairs Officer.

Dudley Knox Library / Naval Postgraduate School
411 Dyer Road / 1 University Circle
Monterey, California USA 93943

<http://www.nps.edu/library>

Discretely Exact Derivatives for Hyperbolic PDE-Constrained Optimization Problems Discretized by the Discontinuous Galerkin Method

Lucas C. Wilcox · Georg Stadler · Tan Bui-Thanh · Omar Ghattas

Received: 27 November 2013 / Revised: 26 May 2014 / Accepted: 10 July 2014
© Springer Science+Business Media New York (outside the USA) 2014

Abstract This paper discusses the computation of derivatives for optimization problems governed by linear hyperbolic systems of partial differential equations (PDEs) that are discretized by the discontinuous Galerkin (dG) method. An efficient and accurate computation of these derivatives is important, for instance, in inverse problems and optimal control problems. This computation is usually based on an adjoint PDE system, and the question addressed in this paper is how the discretization of this adjoint system should relate to the dG discretization of the hyperbolic state equation. Adjoint-based derivatives can either be computed before or after discretization; these two options are often referred to as the optimize-then-discretize and discretize-then-optimize approaches. We discuss the relation between these two options for dG discretizations in space and Runge–Kutta time integration. The influence of different dG formulations and of numerical quadrature is discussed. Discretely exact discretizations for several hyperbolic optimization problems are derived, including the advection equation, Maxwell's equations and the coupled elastic-acoustic wave equation. We find that the discrete adjoint equation inherits a natural dG discretization from the discretization of the state equation and that the expressions for the discretely exact gradient often have to take into

This document has been approved for public release; its distribution is unlimited.

Lucas C. Wilcox (✉)
Department of Applied Mathematics, Naval Postgraduate School,
Monterey, CA, USA
e-mail: lwilcox@nps.edu

G. Stadler · T. Bui-Thanh · O. Ghattas
Institute for Computational Engineering and Sciences,
The University of Texas at Austin, Austin, TX, USA

T. Bui-Thanh
Department of Aerospace Engineering and Engineering Mechanics,
The University of Texas at Austin, Austin, TX, USA

O. Ghattas
Departments of Mechanical Engineering and Jackson School of Geosciences,
The University of Texas at Austin, Austin, TX, USA

account contributions from element faces. For the coupled elastic-acoustic wave equation, the correctness and accuracy of our derivative expressions are illustrated by comparisons with finite difference gradients. The results show that a straightforward discretization of the continuous gradient differs from the discretely exact gradient, and thus is not consistent with the discretized objective. This inconsistency may cause difficulties in the convergence of gradient based algorithms for solving optimization problems.

Keywords Discontinuous Galerkin · PDE-constrained optimization · Discrete adjoints · Elastic wave equation · Maxwell's equations

1 Introduction

Derivatives of functionals, whose evaluation depends on the solution of a partial differential equation (PDE), are required, for instance, in inverse problems and optimal control problems, and play a role in error analysis and a posteriori error estimation. An efficient method to compute derivatives of functionals that require the solution of a state PDE is through the solution of an adjoint equation. In general, this adjoint PDE differs from the state PDE. For instance, for a state equation that involves a first-order time derivative, the adjoint equation must be solved backwards in time.

If the partial differential equation is hyperbolic, the discontinuous Galerkin (dG) method is often a good choice to approximate the solution due to its stability properties, flexibility, accuracy and ease of parallelization. Having chosen a dG discretization for the state PDE, the question arises how to discretize the adjoint equation and the expression for the gradient, and whether and how their discretization should be related to the discretization of the state equation. One approach is to discretize the adjoint equation and the gradient independently from the state equation, possibly leading to inaccurate derivatives as discussed below. A different approach is to derive the discrete adjoint equation based on the discretized state PDE and a discretization of the cost functional. Sometimes this latter approach is called the discretize-then-optimize approach, while the former is known as optimize-then-discretize. For standard Galerkin discretizations, these two possibilities usually coincide; however, they can differ, for instance, for stabilized finite element methods and for shape derivatives [4, 7, 17, 24]. In this paper, we study the interplay between these issues for derivative computation in optimization problems and discretization by the discontinuous Galerkin method.

While computing derivatives through adjoints on the infinite-dimensional level and then discretizing the resulting expressions (optimize-then-discretize) seems convenient, this approach can lead to inaccurate gradients that are not proper derivatives of any optimization problem. This can lead to convergence problems in optimization algorithms due to inconsistencies between the cost functional and gradients [17]. This inaccuracy is amplified when inconsistent gradients are used to approximate second derivatives based on first derivatives, as in quasi-Newton methods such as the BFGS method. Discretizing the PDE and the cost functional first (discretize-then-optimize), and then computing the (discrete) derivatives guarantees consistency. However, when an advanced discretization method is used, computing the discrete derivatives can be challenging. Thus, understanding the relation between discretization and adjoint-based derivative computation is important. In this paper, we compute derivatives based on the discretized equation and then study how the resulting adjoint discretization relates to the dG discretization of the state equation, and study the corresponding consistency issues for the gradient.

Related work: Discretely exact gradients can also be generated via algorithmic differentiation (AD) [16]. While AD guarantees the computation of exact discrete gradients, it is usually slower than hand-coded derivatives. Moreover, applying AD to parallel implementations can be challenging [38]. The notion of *adjoint consistency* for dG (see [1, 20, 21, 33, 35]) is related to the discussion in this paper. Adjoint consistency refers to the fact that the exact solution of the dual (or adjoint) problem satisfies the discrete adjoint equation. This property is important for dG discretizations to obtain optimal-order L^2 -convergence with respect to target functionals. The focus of this paper goes beyond adjoint consistency to consider consistency of the gradient expressions, and considers in what sense the discrete gradient is a discretization of the continuous gradient. For discontinuous Galerkin discretization, the latter aspect is called *dual consistency* in [1]. A systematic study presented in [29] compares different dG methods for linear-quadratic optimal control problems subject to advection-diffusion-reaction equations. In particular, the author targets commutative dG schemes, i.e., schemes for which dG discretization and the gradient derivation commute. Error estimates and numerical experiments illustrate that commutative schemes have desirable properties for optimal control problems.

Contributions: Using example problems, we illustrate that the discrete adjoint of a dG discretization is, again, a dG discretization of the continuous adjoint equation. In particular, an upwind numerical flux for the hyperbolic state equation turns into a downwind flux in the adjoint, which has to be solved backwards in time and converges at the same convergence order as the state equation. We discuss the implications of numerical quadrature and of the choice of the weak or strong form of the dG discretization on the adjoint system. In our examples, we illustrate the computation of derivatives with respect to parameter fields entering in the hyperbolic system either as a coefficient or as forcing terms. Moreover, we show that discretely exact gradients often involve contributions at element faces, which are likely to be neglected in an optimize-then-discretize approach. These contributions are a consequence of the discontinuous basis functions employed in the dG method and since they are at the order of the discretization error, they are particularly important for not fully resolved problems.

Limitations: We restrict ourselves to problems governed by *linear* hyperbolic systems. This allows for an explicit computation of the upwind numerical flux in the dG method through the solution of a Riemann problem. Nonlinear problems often require flux limiting and can develop shocks in the solution. This makes the computation of derivatives problematic since numerical fluxes with limiters are often non-differentiable and defining adjoints when the state solution involves shocks is a challenge [13, 14].

Organization: Next, in Sect. 2, we discuss the interplay of the derivative computation of a cost functional with the spatial and temporal discretization of the governing hyperbolic system; moreover, we discuss the effects of numerical quadrature. For examples of linear hyperbolic systems with increasing complexity we derive the discrete adjoint systems and gradients in Sect. 3, and we summarize important observations. In Sect. 4, we numerically verify our expressions for the discretely exact gradient for a cost functional involving the coupled acoustic-elastic wave equation by comparing to finite differences, and finally, in Sect. 5, we summarize our observations and draw conclusions.

2 Cost Functionals Subject to Linear Hyperbolic Systems

2.1 Problem Formulation

Let $\Omega \subset \mathbb{R}^d$ ($d = 1, 2, 3$) be an open and bounded domain with boundary $\Gamma = \partial\Omega$, and let $T > 0$. We consider the linear n -dimensional hyperbolic system

$$\mathbf{q}_t + \nabla \cdot (\mathbf{F}\mathbf{q}) = \mathbf{f} \quad \text{on } \Omega \times (0, T), \tag{1a}$$

where, for $(\mathbf{x}, t) \in \Omega \times (0, T)$, $\mathbf{q}(\mathbf{x}, t) \in \mathbb{R}^n$ is the vector of state variables and $\mathbf{f}(\mathbf{x}, t) \in \mathbb{R}^n$ is an external force. The flux $\mathbf{F}\mathbf{q} \in \mathbb{R}^{n \times d}$ is linear in \mathbf{q} and the divergence operator is defined as $\nabla \cdot (\mathbf{F}\mathbf{q}) = \sum_{i=1}^d (A_i \mathbf{q})_{x_i}$ with matrix functions $A_i : \Omega \rightarrow \mathbb{R}^{n \times n}$, where the indices denote partial differentiation with respect to x_i . Together with (1a), we assume the boundary and initial conditions

$$B\mathbf{q}(\mathbf{x}, t) = \mathbf{g}(\mathbf{x}, t) \quad \mathbf{x} \in \Gamma, t \in (0, T), \tag{1b}$$

$$\mathbf{q}(\mathbf{x}, 0) = \mathbf{q}_0(\mathbf{x}) \quad \mathbf{x} \in \Omega. \tag{1c}$$

Here, $B : \Gamma \rightarrow \mathbb{R}^{l \times n}$ is a matrix function that takes into account that boundary conditions can only be prescribed on inflow characteristics. Under these conditions, (1) has a unique solution \mathbf{q} in a proper space Q [18].

We target problems, in which the flux, the right hand side, or the boundary or initial condition data in (1) depend on parameters \mathbf{c} from a space U . These parameters can either be finite-dimensional, i.e., $\mathbf{c} = (c_1, \dots, c_k)$ with $k \geq 1$, or infinite-dimensional, e.g., a function $\mathbf{c} = \mathbf{c}(\mathbf{x})$. Examples for functions \mathbf{c} are material parameters such as the wave speed, or the right-hand side forcing in (1a).

Our main interest are inverse and estimation problems, and optimal control problems governed by hyperbolic systems of the form (1). This leads to optimization problems of the form

$$\min_{\mathbf{c}, \mathbf{q}} \tilde{\mathcal{J}}(\mathbf{c}, \mathbf{q}) \quad \text{subject to (1)}, \tag{2}$$

where $\tilde{\mathcal{J}}$ is a cost function that depends on the parameters \mathbf{c} and on the state \mathbf{q} . The parameters \mathbf{c} may be restricted to an admissible set $U_{ad} \subset U$ for instance to incorporate bound constraints. If U_{ad} is chosen such that for each $\mathbf{c} \in U_{ad}$ the state equation (1) admits a unique solution $\mathbf{q} := S(\mathbf{c})$ (where S is the solution operator for the hyperbolic system), then (2) can be written as an optimization problem in \mathbf{c} only, namely

$$\min_{\mathbf{c} \in U_{ad}} \mathcal{J}(\mathbf{c}) := \tilde{\mathcal{J}}(\mathbf{c}, S(\mathbf{c})). \tag{3}$$

Existence and (local) uniqueness of solutions to (2) and (3) depend on the form of the cost function $\tilde{\mathcal{J}}$, properties of the solution and parameter spaces and of the hyperbolic system and have to be studied on a case-to-case basis (we refer, for instance, to [3, 17, 30, 37]). Our main focus is not the solution of the optimization problem (3), but the computation of derivatives of \mathcal{J} with respect to \mathbf{c} , and the interplay of this derivative computation with the spatial and temporal discretization of the hyperbolic system (1). Gradients (and second derivatives) of \mathcal{J} are important to solve (3) efficiently, and can be used for studying parameter sensitivities or quantifying the uncertainty in the solution of inverse problems [6].

2.2 Compatibility of Boundary Conditions

To ensure the existence of a solution to the adjoint equation, compatibility conditions between boundary terms in the cost function $\tilde{\mathcal{J}}$, the boundary operator B in (1b) and the operator \mathbf{F} in (1a) must hold. We consider cost functions of the form

$$\tilde{\mathcal{J}}(\mathbf{c}, \mathbf{q}) = \int_0^T \int_{\Omega} j_{\Omega}(\mathbf{q}) \, dx \, dt + \int_0^T \int_{\Gamma} j_{\Gamma}(C\mathbf{q}) \, dx \, dt + \int_{\Omega} j_T(\mathbf{q}(T)) \, dx,$$

where $j_{\Omega} : \mathbb{R}^n \rightarrow \mathbb{R}$, $j_{\Gamma} : \mathbb{R}^m \rightarrow \mathbb{R}$ and $J_T : \mathbb{R}^n \rightarrow \mathbb{R}$ are differentiable, and $C : \Gamma \rightarrow \mathbb{R}^{m \times n}$ is a matrix-valued function. We denote the derivatives of the functional under the integrals by $j'_{\Omega}(\cdot)$, $j'_{\Gamma}(\cdot)$ and $J'_T(\cdot)$. The Fréchet derivative of \mathcal{J} with respect to \mathbf{q} in a direction $\tilde{\mathbf{q}}$ is given by

$$\begin{aligned} \tilde{\mathcal{J}}_{\mathbf{q}}(\mathbf{c}, \mathbf{q})(\tilde{\mathbf{q}}) &= \int_0^T \int_{\Omega} j'_{\Omega}(\mathbf{q})\tilde{\mathbf{q}} \, dx \, dt + \int_0^T \int_{\Gamma} j'_{\Gamma}(C\mathbf{q})C\tilde{\mathbf{q}} \, dx \, dt \\ &\quad + \int_{\Omega} J'_T(\mathbf{q}(T))\tilde{\mathbf{q}}(T) \, dx. \end{aligned} \tag{4}$$

The boundary operators B and C must be compatible in the sense discussed next. Denoting the outward pointing normal along the boundary Γ by $\mathbf{n} = (n_1, \dots, n_d)^T$, we use the decomposition

$$A := \sum_{i=1}^d n_i A_i = L^T \text{diag}(\lambda_1, \dots, \lambda_n)L, \tag{5}$$

with $L \in \mathbb{R}^{n \times n}$ and $\lambda_1 \geq \dots \geq \lambda_n$. Note that $L^{-1} = L^T$ if A is symmetric. The positive eigenvalues $\lambda_1, \dots, \lambda_s$, correspond to the $s \geq 0$ incoming characteristics, and the negative eigenvalues $\lambda_{n-m+1}, \dots, \lambda_n$ to the $m \geq 0$ outgoing characteristics. Here, we allow for the zero eigenvalues $\lambda_{s+1} = \dots = \lambda_{n-m} = 0$. To ensure well-posedness of the hyperbolic system (1), the initial values of \mathbf{q} can only be specified along incoming characteristics. The first s rows corresponding to incoming characteristics can be identified with the boundary operator B in (1b). To guarantee well-posedness of the adjoint equation, C has to be chosen such that the cost functional $\tilde{\mathcal{J}}$ only involves boundary measurements for outgoing characteristics. These correspond to the rows of L with negative eigenvalues and have to correspond to the boundary operator C . It follows from (5) that

$$A = \begin{bmatrix} B \\ O \\ C \end{bmatrix}^{-1} \begin{pmatrix} \lambda_1 & & \\ & \ddots & \\ & & \lambda_n \end{pmatrix} \begin{bmatrix} B \\ O \\ C \end{bmatrix} = \bar{C}^T B - \bar{B}^T C, \tag{6}$$

where $O \in \mathbb{R}^{(n-s-m) \times n}$ and $\bar{B} \in \mathbb{R}^{l \times n}$, $\bar{C} \in \mathbb{R}^{m \times n}$ are derived properly. If A is symmetric, then $\bar{C}^T = B^T \text{diag}(\lambda_1, \dots, \lambda_s)$, and $\bar{B}^T = -C^T \text{diag}(\lambda_{n-m+1}, \dots, \lambda_n)$. As will be shown in the next section, the matrix \bar{B} is the boundary condition matrix for the adjoint equation. For a discussion of compatibility between the boundary term in a cost functional and hyperbolic systems in a more general context we refer to [1, 12, 21]. In the next section, we formally derive the infinite-dimensional adjoint system and derivatives of the cost functional $\tilde{\mathcal{J}}$.

2.3 Infinite-Dimensional Derivatives

For simplicity, we assume that only the flux \mathbf{F} (i.e., the matrices A_1, A_2, A_3) depend on \mathbf{c} , but B, C, \mathbf{f} and \mathbf{q}_0 do not depend on the parameters \mathbf{c} . We use the formal Lagrangian method

[3,37], in which we consider \mathbf{c} and \mathbf{q} as independent variables and introduce the Lagrangian function

$$\mathcal{L}(\mathbf{c}, \mathbf{q}, \mathbf{p}) := \tilde{\mathcal{J}}(\mathbf{c}, \mathbf{q}) + \int_0^T \int_{\Omega} (\mathbf{q}_t + \nabla \cdot (\mathbf{F}\mathbf{q}) - \mathbf{f}, \mathbf{p})_W \, dx \, dt \tag{7}$$

with $\mathbf{p}, \mathbf{q} \in Q$, where \mathbf{q} satisfies the boundary and initial conditions (1b) and (1c), \mathbf{p} satisfies homogeneous versions of these conditions, and $\mathbf{c} \in U_{ad}$. Here, $(\cdot, \cdot)_W$ denotes a W -weighted inner product in \mathbb{R}^n , with a symmetric positive definite matrix $W \in \mathbb{R}^{n \times n}$ (which may depend on \mathbf{x}). The matrix W can be used to make a hyperbolic system symmetric with respect to the W -weighted inner product, as for instance in the acoustic and coupled elastic-acoustic wave examples discussed in Sects. 3.2 and 3.4. In particular, this gives the adjoint equation a form very similar to the state equation. If boundary conditions depend on the parameters \mathbf{c} , they must be enforced weakly through a Lagrange multiplier in the Lagrangian function and cannot be added in the definition of the solution space for \mathbf{q} . For instance, if the boundary operator $B = B(\mathbf{c})$ depends on \mathbf{c} , the boundary condition (1b) must be enforced weakly through a Lagrange multiplier, amounting to an additional term in the Lagrangian functional (7).

Following the Lagrangian approach [3,37], the gradient of \mathcal{J} coincides with the gradient of \mathcal{L} with respect to \mathbf{c} , provided all variations of \mathcal{L} with respect to \mathbf{q} and \mathbf{p} vanish. Requiring that variations with respect to \mathbf{p} vanish, we recover the state equation. Variations with respect to \mathbf{q} in directions $\tilde{\mathbf{q}}$, that satisfy homogeneous versions of the initial and boundary conditions (1b) and (1c), result in

$$\begin{aligned} \mathcal{L}_{\mathbf{q}}(\mathbf{c}, \mathbf{q}, \mathbf{p})(\tilde{\mathbf{q}}) &= \tilde{\mathcal{J}}_{\mathbf{q}}(\mathbf{c}, \mathbf{q})(\tilde{\mathbf{q}}) - \int_0^T \int_{\Omega} (\mathbf{p}_t, W\tilde{\mathbf{q}}) + (\mathbf{F}\tilde{\mathbf{q}}, \nabla(W\mathbf{p})) \, dx \, dt \\ &\quad + \int_{\Omega} (\tilde{\mathbf{q}}(T), W\mathbf{p}(T)) \, dx + \int_0^T \int_{\Gamma} (\mathbf{n} \cdot \mathbf{F}\tilde{\mathbf{q}}, W\mathbf{p}) \, dx \, dt, \end{aligned}$$

where we have used integration by parts in time and space. As will be discussed in Sect. 2.5, integration by parts can be problematic when integrals are approximated using numerical quadrature and should be avoided to guarantee exact computation of discrete derivatives. In this section, we assume continuous functions \mathbf{q}, \mathbf{p} and exact computation of integrals. Since $\mathbf{n} \cdot \mathbf{F} = A$, (6) implies that

$$\int_0^T \int_{\Gamma} (\mathbf{n} \cdot \mathbf{F}\tilde{\mathbf{q}}, W\mathbf{p}) \, dx \, dt = \int_0^T \int_{\Gamma} (C\tilde{\mathbf{q}}, \bar{B}W\mathbf{p}) - (B\tilde{\mathbf{q}}, \bar{C}W\mathbf{p}) \, dx \, dt.$$

Using the explicit form of the cost given in (4), and that all variations with respect to arbitrary $\tilde{\mathbf{q}}$ that satisfy $B\tilde{\mathbf{q}} = 0$ must vanish, we obtain

$$W\mathbf{p}_t + \mathbf{F}^* \nabla(W\mathbf{p}) = j'_{\Omega}(\mathbf{q}) \quad \text{on } \Omega \times (0, T), \tag{8a}$$

$$\bar{B}W\mathbf{p}(\mathbf{x}, t) = -j'_{\Gamma}(C\mathbf{q}(\mathbf{x}, t)) \quad \mathbf{x} \in \Gamma, t \in (0, T), \tag{8b}$$

$$W\mathbf{p}(\mathbf{x}, T) = -j'_T(\mathbf{q}(\mathbf{x}, T)) \quad \mathbf{x} \in \Omega. \tag{8c}$$

Here, \mathbf{F}^* is the adjoint of \mathbf{F} with respect to the Euclidean inner product. Note that the adjoint system (8) is a final value problem and thus is usually solved backwards in time. Note that, differently from the state system, the adjoint system is not in conservative form.

Next we compute variations of \mathcal{L} with respect to the parameters \mathbf{c} and obtain for variations $\tilde{\mathbf{c}}$ that

$$\mathcal{L}_{\mathbf{c}}(\mathbf{c}, \mathbf{q}, \mathbf{p})(\tilde{\mathbf{c}}) = \int_0^T \int_{\Omega} (\nabla \cdot (\mathbf{F}_{\mathbf{c}}(\tilde{\mathbf{c}})\mathbf{q}), \mathbf{p})_W \, dx \, dt = \int_0^T \int_{\Omega} \sum_{i=1}^d ((A_{i\mathbf{c}}(\tilde{\mathbf{c}})\mathbf{q})_{x_i}, \mathbf{p})_W \, dx \, dt. \tag{9a}$$

Since \mathbf{q} and \mathbf{p} are assumed to solve the state and adjoint system,

$$\mathcal{J}(\mathbf{c})(\tilde{\mathbf{c}}) = \mathcal{L}_{\mathbf{c}}(\mathbf{c}, \mathbf{q}, \mathbf{p})(\tilde{\mathbf{c}}), \text{ where } \mathbf{q} \text{ solves (1) and } \mathbf{p} \text{ solves (8).}$$

Next, we present the dG discretization of the hyperbolic system (1) and discuss the interaction between discretization and the computation of derivatives.

2.4 Discontinuous Galerkin Discretization

For the spatial discretization of hyperbolic systems such as (1), the discontinuous Galerkin (dG) method has proven to be a favorable choice. In the dG method, we divide the domain Ω into disjoint elements Ω^e , and use polynomials to approximate \mathbf{q} on each element Ω^e . The resulting approximation space is denoted by Q^h , and elements $\mathbf{q}_h \in Q^h$ are polynomial on each element, and discontinuous across elements. Using test functions $\mathbf{p}_h \in Q^h$, dG discretization in space implies that for each element Ω^e

$$\int_{\Omega^e} \left(\frac{\partial}{\partial t} \mathbf{q}_h, W \mathbf{p}_h \right) - (\mathbf{F} \mathbf{q}_h, \nabla(W \mathbf{p}_h)) \, dx + \int_{\Gamma^e} \mathbf{n}^- \cdot ((\mathbf{F} \mathbf{q}_h)^\dagger, W \mathbf{p}_h^-) \, dx = \int_{\Omega^e} (f, W \mathbf{p}_h) \, dx \tag{10}$$

for all times $t \in (0, T)$. Here, (\cdot, \cdot) is the inner product in \mathbb{R}^n and $\mathbb{R}^{d \times n}$ and the symmetric and positive definite matrix W acts as a weighting matrix in this inner product. Furthermore, $(\mathbf{F} \mathbf{q}_h)^\dagger$ is the numerical flux, which connects adjacent elements. The superscript “-” denotes that the inward values are chosen on Γ^e , i.e., the values of the approximation on Ω^e ; the superscript “+” denotes that the outwards values are chosen, i.e., the values of an element $\Omega^{e'}$ that is adjacent to Ω^e along the shared boundary Γ^e . Here, \mathbf{n}^- is the outward pointing normal on element Ω^e . The formulation (10) is often referred to as the *weak form* of the dG discretization [23,25]. The corresponding *strong form* dG discretization is obtained by element-wise integration by parts in space in (10), resulting in

$$\int_{\Omega^e} \left(\frac{\partial}{\partial t} \mathbf{q}_h, W \mathbf{p}_h \right) + (\nabla \cdot \mathbf{F} \mathbf{q}_h, W \mathbf{p}_h) \, dx - \int_{\Gamma^e} \mathbf{n}^- \cdot (\mathbf{F} \mathbf{q}_h^- - (\mathbf{F} \mathbf{q}_h)^\dagger, W \mathbf{p}_h^-) \, dx = \int_{\Omega^e} (f, W \mathbf{p}_h) \, dx \tag{11}$$

for all $t \in (0, T)$. To find a solution to the optimization problem (3), derivatives of \mathcal{J} with respect to the parameters \mathbf{c} must be computed. There are two choices for computing derivatives, namely deriving expressions for the derivatives of the continuous problem (3), and then discretizing these equations, or first discretizing the problem and then computing derivatives of this fully discrete problem. If the latter approach is taken, i.e., the discrete adjoints are computed, the question arises whether the discrete adjoint equation is an approximation of the continuous adjoint and if the discrete adjoint equation is again a dG discretization. Moreover, what are the consequences of choosing the weak or the strong form (10) or (11)? A sketch for the different combinations of discretization and computation of derivatives is also shown in Fig. 1.

2.5 Influence of Numerical Quadrature

In a numerical implementation, integrals are often approximated using numerical quadrature. A fully discrete approach has to take into account the resulting quadrature error; in particular,

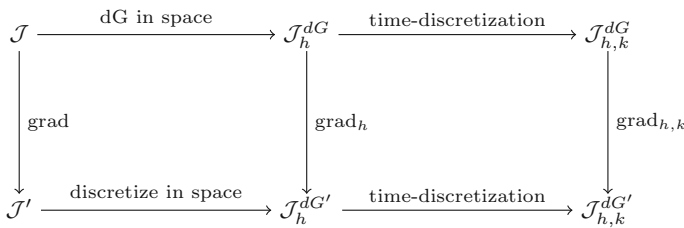


Fig. 1 Sketch to illustrate the relation between discretization of the problem (horizontal arrows, upper row), computation of the gradient with respect to the parameters \mathbf{c} (vertical arrows) and discretization of the gradient (horizontal arrows, lower row). The problem discretization (upper row) requires discretization of the state equation and of the cost functional in space (“dG in space”-arrow) and in time (“time-discretization”-arrow). The vertical arrows represent the Fréchet derivatives of \mathcal{J} (“grad”-arrow), of the semidiscrete cost \mathcal{J}_h^{dG} (“grad_h”-arrow) and the fully discrete cost $\mathcal{J}_{h,k}^{dG}$ (“grad_{h,k}”-arrow). The discretization of the gradient (bottom row) requires space (“discretize in space”-arrow) and time (“time-discretization”-arrow) discretization of the state equation, the adjoint equation and the expression for the gradient. Most of our derivations follow the fully discrete approach, i.e., the upper row and grad_{h,k} arrows; The resulting discrete expressions are then interpreted as discretizations of the corresponding continuous equations derived by following the grad arrow

integration by parts can incur an error in combination with numerical quadrature. Below, we first discuss implications of numerical quadrature in space and then comment on numerical integration in time. In our example problems in Sect. 3, we use integral symbols to denote integration in space and time, but do not assume exact integration. In particular, we avoid integration by parts or highlight when integration by parts is used.

2.5.1 Numerical Integration in Space

The weak form (10) and the strong form (11) of dG are equivalent provided integrals are computed exactly and, as a consequence, integration by parts does not result in numerical error. If numerical quadrature is used, these forms are only numerically equivalent under certain conditions [26]; in general, they are different.

2.5.2 Numerical Integration in Time

We use a method-of-lines approach, that is, from the dG discretization in space we obtain a continuous-in-time system of ordinary differential equations (ODEs), which is then discretized by a Runge–Kutta method. Discrete adjoint equations and the convergence to their continuous counterparts for systems of ODEs discretized by Runge–Kutta methods have been studied, for instance in [19, 39]. For the time-discretization we build on these results.

An alternative approach to discretize time is to use a finite element method, which allows a fully variational formulation of the problem in space-time; we refer, for instance to [2] for this approach applied to parabolic optimization problems.

In both approaches, the computation of derivatives requires the entire time history of both the state and the adjoint solutions. For realistic application problems, storing this entire time history is infeasible, and storage reduction techniques, also known as checkpointing strategies have to be employed. These methods allow one to trade storage against computation time by storing the state solution only at certain time instances, and then recomputing it as needed when solving the adjoint equation and computing the gradient [2, 15, 16].

3 Example Problems

The purpose of this section is to illustrate the issues discussed in the previous sections on example problems. We present examples with increasing complexity and with parameters entering differently in the hyperbolic systems. First, in Sect. 3.1, we derive expressions for derivatives of a functional that depend on the solution of the one-dimensional advection equation. As a simple model problem for hyperbolic equations, we provide extensive details for this example. In particular, we discuss different numerical fluxes. In Sect. 3.2, we compute expressions for the derivatives of a functional with respect to the local wave speed in an acoustic wave equation. This is followed by examples in which we compute derivatives with respect to a boundary forcing in Maxwell's equation (Sect. 3.3) and derivatives with respect to the primary and secondary wave speeds in the coupled acoustic-elastic wave equation (Sect. 3.4). At the end of each example, we summarize our observations in remarks.

Throughout this section, we use the dG discretization introduced in Sect. 2.4 and denote the finite dimensional dG solution spaces by P^h and Q^h . These spaces do not include the boundary conditions which are usually imposed weakly through the numerical flux in the dG method, and they also do not include initial/final time conditions, which we specify explicitly. Functions in these dG spaces are smooth (for instance polynomials) on each element Ω^e and discontinuous across the element boundaries $\partial\Omega^e$. As before, for each element we denote the inward value with a superscript “-” and the outward value with superscript “+”. We use the index h to denote discretized fields and denote by $[[\cdot]]$ the jump, by $[\cdot]$ the difference and by $\{\{\cdot\}\}$ the mean value at an element interface $\partial\Omega^e$. To be precise, for a scalar dG-function u_h , these are defined as $[[u_h]] = u_h^- \mathbf{n}^- + u_h^+ \mathbf{n}^+$, $[u_h] = u_h^- - u_h^+$ and $\{\{u_h\}\} = (u_h^- + u_h^+)/2$. Likewise, for a vector \mathbf{v}_h we define $[[\mathbf{v}_h]] = \mathbf{v}_h^- \cdot \mathbf{n}^- + \mathbf{v}_h^+ \cdot \mathbf{n}^+$, $[\mathbf{v}_h] = \mathbf{v}_h^- - \mathbf{v}_h^+$ and $\{\{\mathbf{v}_h\}\} = (\mathbf{v}_h^- + \mathbf{v}_h^+)/2$ and for a second-order tensor \mathbf{S}_h we have $[[\mathbf{S}_h]] = \mathbf{S}_h^- \mathbf{n}^- + \mathbf{S}_h^+ \mathbf{n}^+$. The domain boundary $\partial\Omega$ is denoted by Γ .

Throughout this section, we use the usual symbol to denote integrals, but we do not assume exact quadrature. Rather, integration can be replaced by a numerical quadrature rule and, as long as the same rule is used throughout, the derivations remain valid. If inexact numerical quadrature is used, integration by parts may not hold exactly; thus, we avoid integration by parts in space, or we point out explicitly when it is used (which is only for the derivation of the strong dG form of the adjoint advection equation (18)). Since our focus is on the spatial dG discretization, we do not discretize the problem in time and assume exact integration in time.

3.1 One-Dimensional Advection Equation

We consider the one-dimensional advection equation on the spatial domain $\Omega = (x_l, x_r) \subset \mathbb{R}$. We assume a spatially varying, continuous positive advection velocity $a(x) \geq a_0 > 0$ for $x \in \Omega$ and a forcing $f(x, t)$ for $(x, t) \in \Omega \times (0, T)$. The advection equation written in conservative form is given by

$$u_t + (au)_x = f \quad \text{on } \Omega \times (0, T), \tag{12a}$$

with the initial condition

$$u(x, 0) = u_0(x) \quad \text{for } x \in \Omega, \tag{12b}$$

and, since $a > 0$, the inflow boundary is $\Gamma_l := \{x_l\}$, where we assume

$$u(x_l, t) = u_l(t) \quad \text{for } t \in (0, T). \tag{12c}$$

The discontinuous Galerkin (dG) method for the numerical solution of (12) in strong form is: Find $u_h \in P^h$ with $u_h(x, 0) = u_0(x), x \in \Omega$ such that for all test functions $p_h \in P^h$ holds

$$\int_{\Omega} (u_{h,t} + (au_h)_x - f)p_h \, dx = \sum_e \int_{\partial\Omega^e} n^- (au_h^- - (au_h)^\dagger) p_h^- \, dx \tag{13}$$

for all $t \in (0, T)$. Here, $a \in U$ can be an infinite-dimensional continuous function, or a finite element function. Note that the integrals on the right hand side in (13) are simple point evaluations; we use the integral notation as it is the common notation that generalizes to two and three-dimensional problems. For $\alpha \in [0, 1]$, the numerical flux on the boundary is replaced by the numerical flux, $(au_h)^\dagger$, given by

$$(au_h)^\dagger = a\{\{u_h\}\} + \frac{1}{2}|a|(1 - \alpha)[[u_h]]. \tag{14}$$

This is a central flux for $\alpha = 1$, and an upwind flux for $\alpha = 0$. Note that in one spatial dimension, the outward normal n is -1 and $+1$ on the left and right side of Ω^e , respectively. Since a is assumed to be continuous on Ω , we have $a^- = a^+ := a$. Moreover, since a is positive, we neglect the absolute value in the following.

As is standard practice [23, 25] we incorporate the boundary conditions weakly through the numerical flux by choosing the “outside” values u_h^+ as $u_h^+ = u_l$ for $x = x_l$ and $u_h^+ = u_h^-$ for $x = x_r$ for the computation of $(au_h)^\dagger$. This implies that $[[u_h]] = n^-(u_h^- - u_l)$ on Γ_l and $[[u_h]] = 0$ on the outflow boundary $\Gamma_r := \{x_r\}$. For completeness, we also provide the dG discretization of (12) in weak form: Find $u_h \in P^h$ with $u_h(x, 0) = u_0(x), x \in \Omega$ such that for all $p_h \in P^h$ holds

$$\int_{\Omega} (u_{h,t} - f)p_h - au_h p_{h,x} \, dx = - \sum_e \int_{\partial\Omega^e} n^- (au_h)^\dagger p_h^- \, dx$$

for all $t \in (0, T)$, which is found by element-wise integration by parts in (13).

Adding the boundary contributions in (13) from adjacent elements Ω^e and $\Omega^{e'}$ to their shared point $\partial\Omega^e \cap \partial\Omega^{e'}$, we obtain

$$\frac{1}{2}|a|(\alpha - 1)[[u_h]][[p_h]] + a[[u_h]]\{\{p_h\}\}.$$

Thus, (13) can also be written as

$$\begin{aligned} \int_{\Omega} (u_{h,t} + (au_h)_x - f)p_h \, dx &= \sum_e \int_{\partial\Omega^e \setminus \Gamma} n^- \left(a\{\{p_h\}\} + a\frac{1}{2}(\alpha - 1)[[p_h]] \right) u_h^- \, dx \\ &\quad + \int_{\Gamma_l} n^- \left(a\frac{1}{2}p_h^- + a\frac{1}{2}(\alpha - 1)n^- p_h^- \right) (u_h^- - u_l) \, dx. \end{aligned} \tag{15}$$

We consider an objective functional for the advection velocity $a \in U$ given by

$$\mathcal{J}(a) := \tilde{\mathcal{J}}(a, u_h) = \int_0^T \int_{\Omega} j_{\Omega}(u_h) \, dx \, dt + \int_0^T \int_{\Gamma} j_{\Gamma}(u_h) \, dx \, dt + \int_{\Omega} r(a) \, dx, \tag{16}$$

with differentiable functions $j_{\Omega} : \Omega \rightarrow \mathbb{R}, j_{\Gamma} : \Gamma \rightarrow \mathbb{R}$ and $r : \Omega \rightarrow \mathbb{R}$. To illustrate compatibility issues as discussed in Sect. 2.2, we define the boundary term in the cost on both the inflow and the outflow part of the boundary; the consequences of this choice are discussed in Remark 1 at the end of this section. To derive the discrete gradient of \mathcal{J} , we use

the Lagrangian function $\mathcal{L} : U \times P^h \times P^h \rightarrow \mathbb{R}$, which combines the cost (16) with the dG discretization (15):

$$\begin{aligned} \mathcal{L}(a, u_h, p_h) &:= \tilde{\mathcal{J}}(a, u_h) + \int_0^T \int_{\Omega} (u_{h,t} + (au_h)_x - f) p_h \, dx \, dt \\ &\quad - \sum_e \int_0^T \int_{\partial\Omega^e \setminus \Gamma} n^- \left(a\{\{p_h\}\} + a\frac{1}{2}(\alpha - 1)\llbracket p_h \rrbracket \right) u_h^- \, dx \, dt \\ &\quad - \int_0^T \int_{\Gamma_l} n^- \left(a\frac{1}{2}p_h^- + a\frac{1}{2}(\alpha - 1)n^- p_h^- \right) (u_h^- - u_l) \, dx \, dt. \end{aligned}$$

By requiring that all variations with respect to p_h vanish, we recover the state equation (15). Variations with respect to u_h in a direction \tilde{u}_h , which satisfies the homogeneous initial conditions $\tilde{u}_h(x, 0) = 0$ for $x \in \Omega$ result in

$$\begin{aligned} \mathcal{L}_{u_h}(a, u_h, p_h)(\tilde{u}_h) &= \int_0^T \int_{\Omega} j'_{\Omega}(u_h)\tilde{u}_h - p_{h,t}\tilde{u}_h + (a\tilde{u}_h)_x p_h \, dx \, dt + \int_{\Omega} p_h(x, T)\tilde{u}_h(x, T) \, dx \\ &\quad - \sum_e \int_0^T \int_{\partial\Omega^e \setminus \Gamma} n^- \left(a\{\{p_h\}\} + a\frac{1}{2}(\alpha - 1)\llbracket p_h \rrbracket \right) \tilde{u}_h^- \, dx \, dt + \int_0^T \int_{\Gamma} j'_{\Gamma}(u_h)\tilde{u}_h \, dx \, dt \\ &\quad - \int_0^T \int_{\Gamma_l} n^- \left(a\frac{1}{2}p_h^- + a\frac{1}{2}(\alpha - 1)n^- p_h^- \right) \tilde{u}_h^- \, dx \, dt. \end{aligned}$$

Since we require that arbitrary variations with respect to u_h must vanish, p_h has to satisfy $p_h(x, T) = 0$ for all $x \in \Omega$, and

$$\begin{aligned} \int_{\Omega} -p_{h,t}\tilde{u}_h + (a\tilde{u}_h)_x p_h + j'_{\Omega}(u_h)\tilde{u}_h \, dx &= \sum_e \int_{\partial\Omega^e \setminus \Gamma_l} n^- (ap_h)^{\dagger} \tilde{u}_h^- \, dx \\ &\quad + \int_{\Gamma_l} n^- \left(\frac{a(2 - \alpha)}{2} p_h^- + j'_{\Gamma}(u_h) \right) \tilde{u}_h^- \, dx \end{aligned} \tag{17a}$$

for all $t \in (0, T)$ and for all \tilde{u}_h , with the adjoint flux

$$(ap_h)^{\dagger} := a\{\{p_h\}\} + \frac{1}{2}a(\alpha - 1)\llbracket p_h \rrbracket \tag{17b}$$

and with

$$p_h^+ := -\frac{j'_{\Gamma}(u_h)}{a(1 - \frac{\alpha}{2})} - \frac{\alpha}{2 - \alpha} p_h^- \quad \text{on } \Gamma_r. \tag{17c}$$

The outside value p_h^+ in (17c) is computed such that $n^-(ap_h)^{\dagger} = j'_{\Gamma}(u_h)$ on Γ_r . Eq. (17) is the weak form of a discontinuous Galerkin discretization of the adjoint equation, with flux given by (17b). An element-wise integration by parts in space in (17a), results in the corresponding strong form of the discrete adjoint equation:

$$\begin{aligned} \int_{\Omega} (-p_{h,t} - ap_{h,x} + j'_{\Omega}(u_h))\tilde{u}_h \, dx &= -\sum_e \int_{\partial\Omega^e \setminus \Gamma_l} n^- (ap_h^- - (ap_h)^{\dagger}) \tilde{u}_h^- \, dx \\ &\quad + \int_{\Gamma_l} n^- \left(-\frac{a\alpha}{2} p_h^- + j'_{\Gamma}(u_h) \right) \tilde{u}_h^- \, dx. \end{aligned} \tag{18}$$

Note that this integration by parts is not always exact if numerical quadrature is used. It can be avoided if the dG weak form of the adjoint equation (17) is implemented directly.

Provided u_h and p_h are solutions to the state and adjoint equations, respectively, the gradient of \mathcal{J} with respect to a is found by taking variations of the Lagrangian with respect to a in a direction \tilde{a} :

$$\begin{aligned} \mathcal{L}_a(a, u_h, p_h)(\tilde{a}) &= \int_{\Omega} r'(a)\tilde{a} \, dx + \int_0^T \int_{\Omega} (\tilde{a}u_h)_x p_h \, dx \, dt \\ &\quad - \sum_e \int_0^T \int_{\partial\Omega^e \setminus \Gamma} n^- \tilde{a} \left(\frac{1}{2}(\alpha - 1)[[p_h]] + \{\{p_h\}\} \right) u_h^- \, dx \, dt \\ &\quad - \int_0^T \int_{\Gamma_l} n^- \tilde{a} \left(\frac{1}{2}(\alpha - 1)n^- p_h^- + \frac{1}{2}p_h^- \right) (u_h^- - u_l) \, dx \, dt. \end{aligned}$$

Thus, the gradient of \mathcal{J} is given by

$$\mathcal{J}'(a)(\tilde{a}) = \int_{\Omega} r'(a)\tilde{a} \, dx + \int_0^T \int_{\Omega} G\tilde{a} \, dx \, dt + \sum_f \int_0^T \int_f g\tilde{a} \, dx \, dt, \tag{19}$$

where G is defined for each element Ω^e , and g for each inter-element face as follows:

$$G\tilde{a} = p_h(\tilde{a}u_h)_x \quad \text{and} \quad g = \begin{cases} \frac{1}{2}(\alpha - 1)[[u_h]][[p_h]] + [[u_h]]\{\{p_h\}\} & \text{if } f \not\subset \Gamma, \\ \frac{1}{2}\alpha p_h^-(u_h^- - u_l) & \text{if } f \subset \Gamma_l, \\ 0 & \text{if } f \subset \Gamma_r. \end{cases}$$

Note that the element boundary jump terms arising in $\mathcal{J}'(a)$ are a consequence of using the dG method to discretize the state equation. While in general these terms do not vanish, they become small as the discretization resolves the continuous state and adjoint variables. However, these terms must be taken into account to compute discretely exact gradients. We continue with a series of remarks:

Remark 1 Only dG discretizations based on upwind fluxes at the boundary can be used in adjoint calculus. This can be seen from the boundary conditions for the adjoint variable p_h , which are weakly imposed through the adjoint numerical flux. Namely, the adjoint variable satisfies the Dirichlet conditions $ap_h(x_r) = -j'_r(u)$ at Γ_r , which, due to the sign change for the advection term in (17) and (18), is an inflow boundary for the adjoint equation. At the (adjoint) outflow boundary Γ_l , the adjoint scheme can only be stable if $j_r|_{\Gamma_l} \equiv 0$. This corresponds to the discussion from Sect. 2.2 on the compatibility of boundary operators. The discrete adjoint scheme is thus consistent (in the sense that the continuous adjoint variable p satisfies the discrete adjoint equation (17)) when $\alpha = 0$, i.e., for a dG scheme based on an upwind numerical flux. Hence, in the following we restrict ourselves to upwind fluxes.

Remark 2 While the dG discretization of the state equation is in conservative form, the discrete adjoint equation is not. Moreover, using the strong form of the dG method for the state system, the adjoint system is naturally a dG method in weak form (see (17)), and element-wise integration by parts is necessary to find the adjoint in strong form (18). Vice versa, using the weak form of dG for the state equation, the adjoint equation is naturally in strong form. These two forms can be numerically different if the integrals are approximated through a quadrature rule for which integration by parts does not hold exactly. In this case, integration by parts should be avoided to obtain exact discrete derivatives.

Remark 3 The numerical fluxes (14) and (17b) differ by the sign in the upwinding term only. Thus, an upwinding flux for the state equation becomes a downwinding flux for the adjoint equation. This is natural since the advection velocity for the adjoint equation is $-a$, which makes the adjoint numerical flux an upwind flux for the adjoint equation.

Remark 4 Computing the continuous adjoint equations and the gradient expression for (16) together with (12) results in the adjoint equation

$$-p_t - ap_x = -j'_\Omega(u) \quad \text{on } \Omega \times (0, T), \tag{20a}$$

$$p(x, T) = 0 \quad \text{for } x \in \Omega, \tag{20b}$$

$$p(x_r, t) = -j'_\Gamma(u) \quad \text{for } t \in (0, T), \tag{20c}$$

and in the gradient expression

$$\mathcal{J}'(a)(\tilde{a}) = \int_\Omega r'(a)\tilde{a} \, dx + \int_0^T \int_\Omega p(\tilde{a}u)_x \, dx \, dt.$$

In an optimize-then-discretize approach, one can freely decide on how to discretize (20) and (4). While (17) or (18) are natural dG-discretizations of (20), a discretization of (4) is likely to neglect the contributions from the element boundaries occurring in (19).

3.2 Acoustic Wave Equation

Next, we derive expressions for the discrete gradient with respect to the local wave speed in the acoustic wave equation. This is important, for instance, in seismic inversion using full wave forms [9,11,28,34]. If the dG method is used to discretize the wave equation (as, e.g., in [5,6,8]), the question on the proper discretization of the adjoint equation and of the expressions for the derivatives arises. Note that in Sect. 3.4 we present the discrete derivatives with respect to the (possibly discontinuous) primary and secondary wave speeds in the coupled acoustic-elastic wave equation, generalizing the results presented in this section. However, for better readability we choose to present this simpler case first and then present the results for the coupled acoustic-elastic equation in compact form in Sect. 3.4.

We consider the acoustic wave equation written as first-order system as follows:

$$e_t - \nabla \cdot \mathbf{v} = 0 \quad \text{on } \Omega \times (0, T), \tag{21a}$$

$$\rho \mathbf{v}_t - \nabla(\lambda e) = \mathbf{f} \quad \text{on } \Omega \times (0, T), \tag{21b}$$

where \mathbf{v} is the velocity, e the dilatation (trace of the strain tensor), $\rho = \rho(\mathbf{x})$ is the mass density and $\lambda = c^2\rho$, where $c(\mathbf{x})$ denotes the wave speed. Together with (21a) and (21b), we assume the initial conditions

$$e(\mathbf{x}, 0) = e_0(\mathbf{x}), \quad \mathbf{v}(\mathbf{x}, 0) = \mathbf{v}_0(\mathbf{x}) \quad \text{for } \mathbf{x} \in \Omega, \tag{21c}$$

and the boundary conditions

$$e(\mathbf{x}, t) = e_{bc}(\mathbf{x}, t), \quad \mathbf{v}(\mathbf{x}, t) = \mathbf{v}_{bc}(\mathbf{x}, t) \quad \text{for } (\mathbf{x}, t) \in \Gamma \times (0, T). \tag{21d}$$

Note that the dG method discussed below uses an upwind numerical flux, and thus the boundary conditions (21) are automatically only imposed at inflow boundaries. Through proper choice of e_{bc} and \mathbf{v}_{bc} classical wave equation boundary conditions can be imposed, e.g., [10,40]. The choice of the dilatation e together with the velocity \mathbf{v} in the first order system formulation is motivated from the strain-velocity formulation used for the coupled elastic and acoustic wave equation in Sect. 3.4.

The strong form dG discretization of (21) is: Find $(e_h, \mathbf{v}_h) \in P^h \times Q^h$ satisfying the initial conditions (21c) such that for all test functions $(h_h, \mathbf{w}_h) \in P^h \times Q^h$ and for all $t \in (0, T)$ holds:

$$\begin{aligned} & \int_{\Omega} (e_{t,h} - \nabla \cdot \mathbf{v}_h) \lambda h_h \, dx + \int_{\Omega} (\rho \mathbf{v}_{t,h} - \nabla(\lambda e_h) - \mathbf{f}) \cdot \mathbf{w}_h \, dx \\ &= - \sum_e \int_{\partial\Omega^e} \mathbf{n}^- \cdot (\mathbf{v}_h^- - \mathbf{v}_h^\dagger) \lambda h_h^- + ((\lambda e_h)^- - (\lambda e_h)^\dagger) \mathbf{n}^- \cdot \mathbf{w}_h^- \, dx. \end{aligned} \quad (22)$$

Note that above, the inner product used for (21a) is weighted by λ , which makes the first-order form of the wave equation a symmetric operator and also allows for a natural interpretation of the adjoint variables, as shown below. Assuming that c and ρ are continuous, we obtain the upwind numerical fluxes:

$$\mathbf{n}^- \cdot \mathbf{v}_h^\dagger = \mathbf{n}^- \cdot \{\{\mathbf{v}_h\}\} - \frac{c}{2} [e_h], \quad (23a)$$

$$(\lambda e_h)^\dagger = \lambda \{\{e_h\}\} - \frac{\rho c}{2} \llbracket \mathbf{v}_h \rrbracket. \quad (23b)$$

Adding the boundary contributions from two adjacent elements Ω^e and $\Omega^{e'}$ in (22) to a shared edge (in 2D) or face (in 3D), one obtains

$$\lambda \llbracket \mathbf{v}_h \rrbracket \{\{h_h\}\} + \frac{c\lambda}{2} [e_h] \llbracket h_h \rrbracket + \frac{\rho c}{2} \llbracket \mathbf{v}_h \rrbracket \llbracket \mathbf{w}_h \rrbracket + \lambda \llbracket e_h \rrbracket \cdot \{\{\mathbf{w}_h\}\}.$$

We compute the discrete gradient with respect to the wave speed c for a cost functional of the form

$$\tilde{\mathcal{J}}(c, \mathbf{v}_h) = \int_0^T \int_{\Omega} j_{\Omega}(\mathbf{v}_h) \, dx \, dt + \int_0^T \int_{\Gamma} j_{\Gamma}(\mathbf{v}_h) \, dx \, dt + \int_{\Omega} r(c) \, dx, \quad (24)$$

with differentiable functions $j_{\Omega} : \Omega \rightarrow \mathbb{R}$, $j_{\Gamma} : \Gamma \rightarrow \mathbb{R}$ and $r : \Omega \rightarrow \mathbb{R}$. To ensure compatibility as discussed in Sect. 2.2, the boundary term j_{Γ} in (24) can only involve outgoing characteristics. We introduce the Lagrangian function, use that all its variations with respect to \mathbf{v} and e must vanish and integrate by parts in time t , resulting in the following adjoint equation: Find $(h_h, \mathbf{w}_h) \in P^h \times Q^h$ satisfying the final time conditions $h(\mathbf{x}, T) = 0$, $\mathbf{w}(\mathbf{x}, T) = 0$ for $\mathbf{x} \in \Omega$, such that for all test functions $(\tilde{e}_h, \tilde{\mathbf{v}}_h) \in P^h \times Q^h$ and for all $t \in (0, T)$ holds:

$$\begin{aligned} & \int_{\Omega} -\tilde{e}_h \lambda h_{h,t} - \nabla \cdot \tilde{\mathbf{v}}_h \lambda h_h - \rho \tilde{\mathbf{v}}_h \cdot \mathbf{w}_{h,t} - \nabla(\lambda \tilde{e}_h) \cdot \mathbf{w}_h + j'_{\Omega}(\mathbf{v}_h) \cdot \tilde{\mathbf{v}}_h \, dx \\ &= - \sum_e \int_{\partial\Omega^e} (\mathbf{n}^- \cdot \mathbf{w}_h^\dagger) \lambda \tilde{e}_h^- + (\lambda h_h)^\dagger \mathbf{n}^- \cdot \tilde{\mathbf{v}}_h^- \, dx - \int_{\Gamma} j'_{\Gamma}(\mathbf{v}_h) \cdot \tilde{\mathbf{v}}_h \, dx, \end{aligned} \quad (25)$$

where the adjoint numerical fluxes are given by

$$\mathbf{n}^- \cdot \mathbf{w}_h^\dagger = \mathbf{n}^- \cdot \{\{\mathbf{w}_h\}\} + \frac{c}{2} [h_h], \quad (26a)$$

$$(\lambda h_h)^\dagger = \lambda \{\{h_h\}\} + \frac{\rho c}{2} \llbracket \mathbf{w}_h \rrbracket. \quad (26b)$$

Note that (25) is the weak form of the dG discretization for an acoustic wave equation, solved backwards in time. This is a consequence of the symmetry of the differential operator in the acoustic wave equation, when considered in the appropriate inner product. Comparing (26) and (23) shows that the adjoint numerical flux (26) is the downwind flux in the adjoint variables for the adjoint wave equation. The strong dG form corresponding to (25) can be obtained by element-wise integration in parts in space.

Finally, we present expressions for the derivative of \mathcal{J} with respect to the wave speed c , which are found as variations of the Lagrangian with respect to c . This results in

$$\mathcal{J}'(c)(\tilde{c}) = \int_{\Omega} r'(c)\tilde{c} \, d\mathbf{x} + \int_0^T \int_{\Omega} G\tilde{c} \, d\mathbf{x} \, dt + \sum_f \int_0^T \int_f g\tilde{c} \, d\mathbf{x} \, dt, \tag{27}$$

where G is defined on each element Ω^e , and g for each inter-element face f as follows:

$$G\tilde{c} = -2\nabla(\rho c \tilde{c} e_h) \cdot \mathbf{w}_h + 2\rho c \tilde{c}(e_{h,t} - \nabla \cdot \mathbf{v}_h)h_h, \tag{28a}$$

$$g = 2\rho c \llbracket \mathbf{v}_h \rrbracket \{ \{ h_h \} \} + \frac{3}{2} \rho c^2 [e_h] [h_h] + \frac{1}{2} \rho \llbracket \mathbf{v}_h \rrbracket \llbracket \mathbf{w}_h \rrbracket + 2\rho c \llbracket e_h \rrbracket \cdot \{ \{ \mathbf{w}_h \} \} \tag{28b}$$

Above, (\mathbf{v}_h, e_h) is the solution of the state equation (22) and (\mathbf{w}_h, h_h) the solution of the adjoint equation (25). Since the state equation (21) is satisfied in the dG sense, (28) simplifies provided $\rho c \tilde{c} h_h \in P^h$, or if a quadrature method is used in which the values of $\rho c \tilde{c} h_h$ at the quadrature points coincide with the values of a function in P^h at these points. The latter is, for instance, always the case when the same nodes are used for the quadrature and the nodal basis. Then, (28) simplifies to

$$G\tilde{c} = -2\nabla(\rho c \tilde{c} e_h) \cdot \mathbf{w}_h, \tag{29a}$$

$$g = \frac{1}{2} \rho c^2 [e_h] [h_h] + \frac{1}{2} \rho \llbracket \mathbf{v}_h \rrbracket \llbracket \mathbf{w}_h \rrbracket + 2\rho c \llbracket e_h \rrbracket \cdot \{ \{ \mathbf{w}_h \} \}. \tag{29b}$$

As for the one-dimensional advection problem (see Remark 3), the upwind flux in the state equation becomes a downwind flux in the adjoint equation, and thus an upwind flux for the adjoint equation when solved backwards in time.

Remark 5 As in the advection example, the discrete gradient has boundary contributions that involve jumps of the dG variables at the element boundaries [see (28b) and (29b)]. These jumps are at the order of the dG approximation error and thus tend to zero as the dG solution converges to the continuous solution either through mesh refinement or improvement of the approximation on each element.

3.3 Maxwell's Equations

Here we derive expressions for the discrete gradient with respect to the current density in Maxwell's equations (specifically boundary current density in our case). This can be used, for instance, in the determination and reconstruction of antennas from boundary field measurements [32] and controlling electromagnetic fields using currents [27, 41]. The time-dependent Maxwell's equations in a homogeneous isotropic dielectric domain $\Omega \subset \mathbb{R}^3$ is given by:

$$\mu \mathbf{H}_t = -\nabla \times \mathbf{E} \quad \text{on } \Omega \times (0, T), \tag{30a}$$

$$\epsilon \mathbf{E}_t = \nabla \times \mathbf{H} \quad \text{on } \Omega \times (0, T), \tag{30b}$$

$$\nabla \cdot \mathbf{H} = 0 \quad \text{on } \Omega \times (0, T), \tag{30c}$$

$$\nabla \cdot \mathbf{E} = 0 \quad \text{on } \Omega \times (0, T), \tag{30d}$$

where \mathbf{E} is the electric field and \mathbf{H} is the magnetic field. Moreover, μ is the permeability and ϵ is the permittivity, which can both be discontinuous across element interfaces. The impedance Z and the conductance Y of the material are defined as $Z = \frac{1}{Y} = \sqrt{\frac{\mu}{\epsilon}}$. Note that we follow a standard notation for Maxwell's equation, in which the vectors \mathbf{H} and \mathbf{E}

are denoted by bold capital letters. Together with Eqs. (30a)–(30d), we assume the initial conditions

$$\mathbf{E}(\mathbf{x}, 0) = \mathbf{E}_0(\mathbf{x}), \mathbf{H}(\mathbf{x}, 0) = \mathbf{H}_0(\mathbf{x}) \quad \text{on } \Omega, \tag{30e}$$

and boundary conditions

$$\mathbf{n} \times \mathbf{H} = -\mathbf{J}_s \quad \text{on } \Gamma. \tag{30f}$$

This classic boundary condition can be converted to equivalent inflow characteristic boundary conditions [36]. Here, $\mathbf{J}_s(\mathbf{x}, t)$ is a spatially (and possibly time-dependent) current density flowing tangentially to the boundary. If the initial conditions satisfy the divergence conditions (30c) and (30d), the time evolved solution will as well [22]. Thus, the divergence conditions can be regarded as a consistency condition on the initial conditions. We consider a dG discretization of Maxwell’s equations that only involves Eqs. (30a) and (30b) explicitly. The dG solution then satisfies the divergence conditions up to discretization error. The strong form dG discretization of Eq. (30) is: Find $(\mathbf{H}_h, \mathbf{E}_h) \in P^h \times Q^h$ satisfying the initial conditions (30e), such that

$$\begin{aligned} & \int_{\Omega} (\mu \mathbf{H}_{h,t} + \nabla \times \mathbf{E}_h) \cdot \mathbf{G}_h \, d\mathbf{x} + \int_{\Omega} (\epsilon \mathbf{E}_{h,t} - \nabla \times \mathbf{H}_h) \cdot \mathbf{F}_h \, d\mathbf{x} = \\ & \sum_e \int_{\partial\Omega^e} -(\mathbf{n}^- \times (\mathbf{E}_h^\dagger - \mathbf{E}_h^-)) \cdot \mathbf{G}_h \, d\mathbf{x} + \sum_e \int_{\partial\Omega^e} (\mathbf{n}^- \times (\mathbf{H}_h^\dagger - \mathbf{H}_h^-)) \cdot \mathbf{F}_h \, d\mathbf{x} \end{aligned}$$

for all $(\mathbf{G}_h, \mathbf{F}_h) \in P^h \times Q^h$, and for all $t \in (0, T)$. The upwind numerical flux states (see [31]) are

$$\mathbf{n}^- \times (\mathbf{E}_h^\dagger - \mathbf{E}_h^-) = -\frac{1}{2\{\{Y\}\}} \mathbf{n}^- \times (Y^+[\mathbf{E}_h] + \mathbf{n}^- \times [\mathbf{H}_h]), \tag{31a}$$

$$\mathbf{n}^- \times (\mathbf{H}_h^\dagger - \mathbf{H}_h^-) = -\frac{1}{2\{\{Z\}\}} \mathbf{n}^- \times (Z^+[\mathbf{H}_h] - \mathbf{n}^- \times [\mathbf{E}_h]). \tag{31b}$$

The boundary conditions (30f) are imposed via the upwind numerical flux by setting exterior values on the boundary of the domain Γ such that

$$\begin{aligned} \mathbf{H}_h^+ &= -\mathbf{H}_h^- + 2\mathbf{J}_s, \\ \mathbf{E}_h^+ &= \mathbf{E}_h^-, \end{aligned} \tag{32}$$

with the continuously extended material parameters $Y^+ = Y^-$ and $Z^+ = Z^-$. Using the upwind numerical flux implicitly means that the boundary conditions are only set on the incoming characteristics.

Next, we compute the discrete adjoint equation and the gradient with respect to the boundary current density \mathbf{J}_s for an objective functional of the form

$$\tilde{\mathcal{J}}(\mathbf{J}_s, \mathbf{E}_h) = \int_0^T \int_{\Omega} j_{\Omega}(\mathbf{E}_h) \, d\mathbf{x} \, dt + \int_0^T \int_{\Gamma} r(\mathbf{J}_s) \, d\mathbf{x} \, dt,$$

with differentiable functions $j_{\Omega} : \Omega \rightarrow \mathbb{R}$ and $r : \Gamma \rightarrow \mathbb{R}$. We introduce the Lagrangian function, and derive the adjoint equation by imposing that all variations of the Lagrangian with respect to \mathbf{H}_h and \mathbf{E}_h must vanish. After integration by parts in time t , this results in the following adjoint equation: Find $(\mathbf{G}_h, \mathbf{F}_h) \in P^h \times Q^h$ such that

$$\int_{\Omega} \mu \mathbf{G}_{h,t} \cdot \tilde{\mathbf{H}}_h + \mathbf{F}_h \cdot (\nabla \times \tilde{\mathbf{H}}_h) \, dx + \int_{\Omega} \epsilon \mathbf{F}_{h,t} \cdot \tilde{\mathbf{E}}_h - \mathbf{G}_h \cdot (\nabla \times \tilde{\mathbf{E}}_h) \, dx = \sum_e \int_{\partial\Omega^e} -(\mathbf{n}^- \times \mathbf{F}_h^\dagger) \cdot \tilde{\mathbf{H}}_h \, dx + \sum_e \int_{\partial\Omega^e} (\mathbf{n}^- \times \mathbf{G}_h^\dagger) \cdot \tilde{\mathbf{E}}_h \, dx - \int_{\Omega} j'_{\Omega}(\mathbf{E}_h) \cdot \tilde{\mathbf{E}}_h \, dx \tag{33}$$

for all $(\tilde{\mathbf{H}}_h, \tilde{\mathbf{E}}_h) \in P^h \times Q^h$ and all $t \in (0, T)$, with the final time conditions

$$\mathbf{G}_h(\mathbf{x}, T) = 0, \mathbf{F}_h(\mathbf{x}, T) = 0 \quad \text{on } \Omega, \tag{34}$$

and the adjoint numerical flux states

$$\mathbf{F}_h^\dagger = \frac{\{\{Y \mathbf{F}_h\}\}}{\{\{Y\}\}} + \frac{1}{2\{\{Y\}\}} (\mathbf{n}^- \times [\mathbf{G}_h]), \tag{35a}$$

$$\mathbf{G}_h^\dagger = \frac{\{\{Z \mathbf{G}_h\}\}}{\{\{Z\}\}} - \frac{1}{2\{\{Z\}\}} (\mathbf{n}^- \times [\mathbf{F}_h]), \tag{35b}$$

with exterior values on the boundary Γ given by $\mathbf{G}_h^+ = -\mathbf{G}_h^-$ and $\mathbf{F}_h^+ = \mathbf{F}_h^-$. These exterior states enforce the continuous adjoint boundary condition

$$\mathbf{n} \times \mathbf{G} = 0 \quad \text{on } \Gamma.$$

To compare with the numerical flux (31) of the state equation, we rewrite the adjoint numerical flux states as

$$\begin{aligned} \mathbf{n}^- \times (\mathbf{F}_h^\dagger - \mathbf{F}_h^-) &= -\frac{1}{2\{\{Y\}\}} \mathbf{n}^- \times (Y^+[\mathbf{F}_h] - \mathbf{n}^- \times [\mathbf{G}_h]), \\ \mathbf{n}^- \times (\mathbf{G}_h^\dagger - \mathbf{G}_h^-) &= -\frac{1}{2\{\{Z\}\}} \mathbf{n}^- \times (Z^+[\mathbf{G}_h] + \mathbf{n}^- \times [\mathbf{F}_h]). \end{aligned} \tag{36}$$

Note that, even with discontinuities in the material parameters, (33) is the weak form of the dG discretization for a Maxwell's system solved backwards in time. As in the acoustic example, the adjoint numerical flux states (35) come from the downwind flux.

Differentiating the Lagrangian with respect to the boundary current \mathbf{J}_s yields an equation for the derivative in direction $\tilde{\mathbf{J}}_s$, namely

$$\mathcal{J}'(\mathbf{J}_s)(\tilde{\mathbf{J}}_s) = \int_0^T \int_{\Gamma} r'(\mathbf{J}_s) \cdot \tilde{\mathbf{J}}_s \, dx \, dt + \int_0^T \int_{\Gamma} \mathbf{g} \cdot \tilde{\mathbf{J}}_s \, dx \, dt \tag{37a}$$

with

$$\mathbf{g} = \mathbf{n}^- \times \mathbf{F}_h + \frac{1}{Y} (\mathbf{n}^- \times (\mathbf{n}^- \times \mathbf{G}_h)), \tag{37b}$$

where $(\mathbf{G}_h, \mathbf{F}_h)$ is the solution of the discrete adjoint equation (33).

Remark 6 Since the boundary force \mathbf{J}_s enters linearly in Maxwell's equation, the gradient expression (37) does not involve contributions from the element boundaries as for the advection and the acoustic wave example.

3.4 Coupled Elastic-Acoustic Wave Equation

Finally, we present expressions for the derivatives with respect to the primary and secondary wave speeds in the coupled acoustic-elastic wave equation. This section generalizes Sect. 3.2 to the coupled acoustic-elastic wave equation. We derive derivative expressions with respect to both wave speeds, and allow for discontinuous wave speeds across elements. We only present

a condensed form of the derivations, and verify our results for the gradient numerically in Sect. 4.

The coupled linear elastic-acoustic wave equation for isotropic material written in first-order velocity strain form is given as

$$\mathbf{E}_t = \frac{1}{2} (\nabla \mathbf{v} + \nabla \mathbf{v}^T) \quad \text{on } \Omega \times (0, T) \tag{38a}$$

$$\rho \mathbf{v}_t = \nabla \cdot (\lambda \operatorname{tr}(\mathbf{E}) \mathbf{I} + 2\mu \mathbf{E}) + \rho \mathbf{f} \quad \text{on } \Omega \times (0, T) \tag{38b}$$

where \mathbf{E} is the strain tensor, \mathbf{v} is the displacement velocity, \mathbf{I} is the identity tensor, $\rho = \rho(\mathbf{x})$ is the mass density, \mathbf{f} is a body force per unit mass, and $\lambda = \lambda(\mathbf{x})$ and $\mu = \mu(\mathbf{x})$ are the Lamé parameters. In addition to the conditions (38a) and (38b) on the body Ω , we assume the initial conditions

$$\mathbf{v}(0, \mathbf{x}) = \mathbf{v}_0(\mathbf{x}), \mathbf{E}(0, \mathbf{x}) = \mathbf{E}_0(\mathbf{x}), \quad \text{for } \mathbf{x} \in \Omega, \tag{38c}$$

and the boundary conditions

$$\mathbf{S}(\mathbf{x}, t) \mathbf{n} = \mathbf{t}^{\text{bc}}(t) \quad \text{on } \Gamma. \tag{38d}$$

Here, \mathbf{t}^{bc} is the traction on the boundary of the body. The stress tensor \mathbf{S} is related to the strain through the constitutive relation (here, \mathbf{C} is the forth-order constitutive tensor):

$$\mathbf{S} = \mathbf{C}\mathbf{E} = \lambda \operatorname{tr}(\mathbf{E}) \mathbf{I} + 2\mu \mathbf{E},$$

where $\operatorname{tr}(\cdot)$ is the trace operator. There are also boundary conditions at material interfaces. For an elastic-elastic interface Γ^{ee} the boundary conditions are

$$\mathbf{v}^+ = \mathbf{v}^-, \mathbf{S}^+ \mathbf{n}^- = \mathbf{S}^- \mathbf{n}^- \quad \text{on } \Gamma^{\text{ee}} \tag{39}$$

and for acoustic-elastic and acoustic-acoustic interfaces Γ^{ae} , the boundary conditions are

$$\mathbf{n} \cdot \mathbf{v}^+ = \mathbf{n} \cdot \mathbf{v}^-, \mathbf{S}^+ \mathbf{n}^- = \mathbf{S}^- \mathbf{n}^- \quad \text{on } \Gamma^{\text{ae}}. \tag{40}$$

The strong form dG discretization of Eq. (38) is: Find $(\mathbf{E}_h, \mathbf{v}_h) \in P^h \times Q^h$ such that

$$\begin{aligned} & \int_{\Omega} \mathbf{E}_{h,t} : \mathbf{C}\mathbf{H}_h \, dx + \int_{\Omega} \rho \mathbf{v}_{h,t} \cdot \mathbf{w}_h \, dx - \int_{\Omega} \operatorname{sym}(\nabla \mathbf{v}_h) : \mathbf{C}\mathbf{H}_h \, dx \\ & - \int_{\Omega} (\nabla \cdot (\mathbf{C}\mathbf{E}_h) + \mathbf{f}) \cdot \mathbf{w}_h \, dx = \sum_e \int_{\partial\Omega^e} \operatorname{sym}(\mathbf{n}^- \otimes (\mathbf{v}_h^\dagger - \mathbf{v}_h^-)) : \mathbf{C}\mathbf{H}_h \, dx \\ & + \sum_e \int_{\partial\Omega^e} ((\mathbf{C}\mathbf{E}_h)^\dagger - (\mathbf{C}\mathbf{E}_h)^-) \mathbf{n}^- \cdot \mathbf{w}_h \, dx \end{aligned} \tag{41}$$

for all $(\mathbf{H}_h, \mathbf{w}_h) \in P^h \times Q^h$ where sym is the mapping to get the symmetric part of a tensor, i.e., $\operatorname{sym}(\mathbf{A}) = \frac{1}{2} (\mathbf{A} + \mathbf{A}^T)$. Note that the constitutive tensor \mathbf{C} is used in the inner product for the weak form. Here, the upwind states are given such that

$$\begin{aligned} \text{sym} \left(\mathbf{n}^- \otimes (\mathbf{v}_h^\dagger - \mathbf{v}_h^-) \right) &= -k_0 \left(\mathbf{n}^- \cdot \llbracket \mathbf{C} \mathbf{E}_h \rrbracket + \rho^+ c_p^+ \llbracket \mathbf{v}_h \rrbracket \right) (\mathbf{n}^- \otimes \mathbf{n}^-) \\ &\quad + k_1 \text{sym} \left(\mathbf{n}^- \otimes (\mathbf{n}^- \times (\mathbf{n}^- \times \llbracket \mathbf{C} \mathbf{E}_h \rrbracket)) \right) \\ &\quad + k_1 \rho^+ c_s^+ \text{sym} \left(\mathbf{n}^- \otimes (\mathbf{n}^- \times (\mathbf{n}^- \times \llbracket \mathbf{v}_h \rrbracket)) \right), \end{aligned} \tag{42a}$$

$$\begin{aligned} ((\mathbf{C} \mathbf{E}_h)^\dagger - (\mathbf{C} \mathbf{E}_h)^-) \mathbf{n}^- &= -k_0 \left(\mathbf{n}^- \cdot \llbracket \mathbf{C} \mathbf{E}_h \rrbracket + \rho^+ c_p^+ \llbracket \mathbf{v}_h \rrbracket \right) \rho^- c_p^- \mathbf{n}^- \\ &\quad + k_1 \rho^- c_s^- \mathbf{n}^- \times (\mathbf{n}^- \times \llbracket \mathbf{C} \mathbf{E}_h \rrbracket) \\ &\quad + k_1 \rho^+ c_s^+ \rho^- c_s^- \mathbf{n}^- \times (\mathbf{n}^- \times \llbracket \mathbf{v}_h \rrbracket), \end{aligned} \tag{42b}$$

with $k_0 = 1/(\rho^- c_p^- + \rho^+ c_p^+)$ and

$$k_1 = \begin{cases} \frac{1}{\rho^- c_s^- + \rho^+ c_s^+} & \text{when } \mu^- \neq 0, \\ 0 & \text{when } \mu^- = 0, \end{cases}$$

where $c_p := \sqrt{(\lambda + 2\mu)/\rho}$ is the primary wave speed and $c_s := \sqrt{\mu/\rho}$ is the secondary wave speed. The traction boundary conditions are imposed through the upwind numerical flux by setting exterior values on Γ to

$$\begin{aligned} \mathbf{v}_h^+ &= \mathbf{v}_h^-, \\ \mathbf{C}^+ \mathbf{E}_h^+ \mathbf{n}^+ &= \begin{cases} -2\mathbf{t}^{\text{bc}} + \mathbf{C}^- \mathbf{E}_h^- \mathbf{n}^- & \text{if } \mu^- \neq 0, \\ -2(\mathbf{n}^- \cdot (\mathbf{t}^{\text{bc}} - \mathbf{C}^- \mathbf{E}_h^- \mathbf{n}^-)) \mathbf{n}^- - \mathbf{C}^- \mathbf{E}_h^- \mathbf{n}^- & \text{if } \mu^+ = 0, \end{cases} \end{aligned}$$

with the continuously extended material parameters $\rho^+ = \rho^-$, $\mu^+ = \mu^-$, and $\lambda^+ = \lambda^-$.

We assume a cost function that depends on the primary and secondary wave speeds c_p and c_s through the solution \mathbf{v}_h of (41)

$$\mathcal{J}(c_p, c_s) = \int_0^T \int_\Omega j_\Omega(\mathbf{v}_h) \, d\mathbf{x} \, dt + \int_\Omega r_p(c_p) \, d\mathbf{x} + \int_\Omega r_s(c_s) \, d\mathbf{x}.$$

By using a sum of spatial Dirac delta distributions in $j_\Omega(\cdot)$, this can include seismogram data, as common in seismic inversion. Using the Lagrangian function and integration by parts in time, we obtain the following adjoint equation: Find $(\mathbf{H}_h, \mathbf{w}_h) \in P^h \times Q^h$ such that

$$\begin{aligned} \int_\Omega -\mathbf{H}_{h,t} : \mathbf{C} \tilde{\mathbf{E}}_h \, d\mathbf{x} - \int_\Omega \rho \mathbf{w}_{h,t} \cdot \tilde{\mathbf{v}}_h \, d\mathbf{x} - \int_\Omega \mathbf{C} \mathbf{H}_h : \text{sym}(\nabla \tilde{\mathbf{v}}_h) \, d\mathbf{x} \\ - \int_\Omega \mathbf{w}_h \cdot (\nabla \cdot (\mathbf{C} \tilde{\mathbf{E}}_h)) \, d\mathbf{x} = - \sum_e \int_{\partial\Omega^e} \text{sym}(\mathbf{n}^- \otimes \mathbf{w}_h^\dagger) : \mathbf{C} \tilde{\mathbf{E}}_h \, d\mathbf{x} \\ - \sum_e \int_{\partial\Omega^e} ((\mathbf{C} \mathbf{H}_h)^\dagger \mathbf{n}^-) \cdot \tilde{\mathbf{v}}_h \, d\mathbf{x} - \int_\Omega j_\Omega(\mathbf{v}_h) \cdot \tilde{\mathbf{v}}_h \end{aligned} \tag{43}$$

for all $(\tilde{\mathbf{E}}_h, \tilde{\mathbf{v}}_h) \in P^h \times Q^h$ in with final conditions $\mathbf{w}_h(T) = 0$ and $\mathbf{H}_h(T) = 0$ the fluxes are given by (see [40])

$$\begin{aligned} \text{sym} \left(\mathbf{n}^- \otimes \mathbf{w}_h^\dagger \right) &= k_0 \left(\mathbf{n}^- \cdot \llbracket \mathbf{C} \mathbf{H}_h \rrbracket + \mathbf{n}^- \cdot (2\{\{\rho c_p \mathbf{w}_h\}\}) \right) \left(\mathbf{n}^- \otimes \mathbf{n}^- \right) \\ &\quad - k_1 \text{sym} \left(\mathbf{n}^- \otimes \left(\mathbf{n}^- \times \left(\mathbf{n}^- \times \llbracket \mathbf{C} \mathbf{H}_h \rrbracket \right) \right) \right) \\ &\quad - k_1 \text{sym} \left(\mathbf{n}^- \otimes \left(\mathbf{n}^- \times \left(\mathbf{n}^- \times (2\{\{\rho c_s \mathbf{w}_h\}\}) \right) \right) \right), \\ (\mathbf{C} \mathbf{H}_h)^\dagger \mathbf{n}^- &= k_0 \left(\mathbf{n}^- \cdot \left(\left(\rho^+ c_p^+ \mathbf{C}^- \mathbf{H}_h^- + \rho^- c_p^- \mathbf{C}^+ \mathbf{H}_h^+ \right) \mathbf{n}^- \right) + \rho^- c_p^- \rho^+ c_p^+ \llbracket \mathbf{w}_h \rrbracket \right) \mathbf{n}^- \\ &\quad - k_1 \mathbf{n}^- \times \left(\mathbf{n}^- \times \left(\left(\rho^+ c_s^+ \mathbf{C}^- \mathbf{H}_h^- + \rho^- c_s^- \mathbf{C}^+ \mathbf{H}_h^+ \right) \mathbf{n}^- \right) \right) \\ &\quad - k_1 \rho^- c_s^- \rho^+ c_s^+ \mathbf{n}^- \times \left(\mathbf{n}^- \times [\mathbf{w}_h] \right). \end{aligned}$$

We can rewrite this into a form similar to the upwind states of the state equation (42) as

$$\begin{aligned} \text{sym} \left(\mathbf{n}^- \otimes \left(\mathbf{w}_h^\dagger - \mathbf{w}_h^- \right) \right) &= k_0 \left(\mathbf{n}^- \cdot \llbracket \mathbf{C} \mathbf{H}_h \rrbracket - \rho^+ c_p^+ \llbracket \mathbf{w}_h \rrbracket \right) \left(\mathbf{n}^- \otimes \mathbf{n}^- \right) \\ &\quad - k_1 \text{sym} \left(\mathbf{n}^- \otimes \left(\mathbf{n}^- \times \left(\mathbf{n}^- \times \llbracket \mathbf{C} \mathbf{H}_h \rrbracket \right) \right) \right) \\ &\quad + k_1 \rho^+ c_s^+ \text{sym} \left(\mathbf{n}^- \otimes \left(\mathbf{n}^- \times \left(\mathbf{n}^- \times [\mathbf{w}_h] \right) \right) \right), \\ \left((\mathbf{C} \mathbf{H}_h)^\dagger - (\mathbf{C} \mathbf{H}_h)^- \right) \mathbf{n}^- &= k_0 \left(-\mathbf{n}^- \cdot \llbracket \mathbf{C} \mathbf{H}_h \rrbracket + \rho^+ c_p^+ \llbracket \mathbf{w}_h \rrbracket \right) \rho^- c_p^- \mathbf{n}^- \\ &\quad + k_1 \rho^- c_s^- \mathbf{n}^- \times \left(\mathbf{n}^- \times \llbracket \mathbf{C} \mathbf{H}_h \rrbracket \right) \\ &\quad - k_1 \rho^- c_s^- \rho^+ c_s^+ \mathbf{n}^- \times \left(\mathbf{n}^- \times [\mathbf{w}_h] \right). \end{aligned}$$

Here, the adjoint boundary conditions are imposed through the adjoint numerical flux by setting exterior values on Γ to

$$\begin{aligned} \mathbf{w}_h^+ &= \mathbf{w}_h^-, \\ \mathbf{C}^+ \mathbf{H}_h^+ \mathbf{n}^+ &= \begin{cases} \mathbf{C}^- \mathbf{H}_h^- \mathbf{n}^- & \text{if } \mu^- \neq 0, \\ -\mathbf{C}^- \mathbf{H}_h^- \mathbf{n}^- + 2 \left(\mathbf{n}^- \cdot (\mathbf{C}^- \mathbf{H}_h^- \mathbf{n}^-) \right) \mathbf{n}^- & \text{if } \mu^- = 0, \end{cases} \end{aligned}$$

with the continuously extended material parameters $\rho^+ = \rho^-$, $\mu^+ = \mu^-$, and $\lambda^+ = \lambda^-$.

We assume a discretization of c_p and c_s and a numerical quadrature rule such that the state equation can be used to simplify the expression for the gradient; see the discussion in Sect. 3.2. The discrete gradient with respect to c_p is then

$$\mathcal{J}_{c_p}(c_p, c_s)(\tilde{c}_p) = \int_{\Omega} r'_p(c_p) \tilde{c}_p \, dx + \int_0^T \int_{\Omega} G_p \tilde{c}_p \, dx \, dt + \sum_{\partial \Omega^e} \int_0^T \int_{\partial \Omega^e} g_p \tilde{c}_p^- \, dx \, dt, \tag{44a}$$

where G_p is defined on each element Ω^e , and g_p for each element boundary as follows:

$$\begin{aligned} G_p \tilde{c}_p &= -2 \left(\nabla \left(\rho c_p \tilde{c}_p \, \text{tr}(\mathbf{E}_h) \right) \right) \cdot \mathbf{w}_h, \\ g_p &= -k_0^2 \rho^- \mathbf{n}^- \cdot \llbracket \mathbf{C} \mathbf{E}_h \rrbracket \mathbf{n}^- \cdot \llbracket \mathbf{C} \mathbf{H}_h \rrbracket + k_0^2 \rho^- \left(\rho^+ c_p^+ \right)^2 \llbracket \mathbf{v}_h \rrbracket \llbracket \mathbf{w}_h \rrbracket \\ &\quad + k_0^2 \rho^- \rho^+ c_p^+ \left(\mathbf{n}^- \cdot \llbracket \mathbf{C} \mathbf{E}_h \rrbracket \llbracket \mathbf{w}_h \rrbracket - \llbracket \mathbf{v}_h \rrbracket \mathbf{n}^- \cdot \llbracket \mathbf{C} \mathbf{H}_h \rrbracket \right) \\ &\quad + 2k_0 \rho^- c_p^- \, \text{tr}(\mathbf{E}_h^-) \left(\mathbf{n}^- \cdot \llbracket \mathbf{C} \mathbf{H}_h \rrbracket - \rho^+ c_p^+ \llbracket \mathbf{w}_h \rrbracket \right) \\ &\quad + 2\rho^- c_p^- \, \text{tr}(\mathbf{E}_h^-) \mathbf{w}_h^- \cdot \mathbf{n}^-, \end{aligned} \tag{44b}$$

where $(\mathbf{v}_h, \mathbf{E}_h)$ is the solution of the state equation (41) and $(\mathbf{w}_h, \mathbf{H}_h)$ is the solution of the adjoint equation (43). The discrete gradient of \mathcal{J} with respect to c_s is

$$\mathcal{J}_{c_s}(c_p, c_s)(\tilde{c}_s) = \int_{\Omega} r'_s(c_s) \tilde{c}_s \, dx + \int_0^T \int_{\Omega} G_s \tilde{c}_s \, dx \, dt + \sum_{\partial \Omega^e} \int_0^T \int_{\partial \Omega^e} g_s \tilde{c}_s^- \, dx \, dt,$$

where G_s is defined on each element Ω^e , and g_s for each element boundary as follows:

$$\begin{aligned}
 G_s \tilde{c}_s &= -4 (\nabla \cdot (\rho c_s \tilde{c}_s (\mathbf{E}_h - \text{tr}(\mathbf{E}_h) \mathbf{I}))) \cdot \mathbf{w}_h, \\
 g_s &= -k_1^2 \rho^- (\mathbf{n}^- \times (\mathbf{n}^- \times \llbracket \mathbf{C} \mathbf{E}_h \rrbracket)) \cdot (\mathbf{n}^- \times (\mathbf{n}^- \times (\llbracket \mathbf{C} \mathbf{H}_h \rrbracket - \rho^+ c_s^+ [\mathbf{w}_h]))) \\
 &\quad - k_1^2 \rho^- \rho^+ c_s^+ (\mathbf{n}^- \times (\mathbf{n}^- \times [\mathbf{v}_h])) \cdot (\mathbf{n}^- \times (\mathbf{n}^- \times (\llbracket \mathbf{C} \mathbf{H}_h \rrbracket - \rho^+ c_s^+ [\mathbf{w}_h]))) \\
 &\quad + 4k_0 \rho^- c_s^- (\mathbf{n}^- \cdot \mathbf{E}_h^- \mathbf{n}^- - \text{tr}(\mathbf{E}_h^-)) (\mathbf{n}^- \cdot (\llbracket \mathbf{C} \mathbf{H}_h \rrbracket - \rho^+ c_s^+ [\mathbf{w}_h])) \\
 &\quad + 4k_1 \rho^- c_s^- (\mathbf{n}^- \times (\mathbf{n}^- \times (\mathbf{E}_h^- \mathbf{n}^-))) \cdot (\mathbf{n}^- \times (\mathbf{n}^- \times (\llbracket \mathbf{C} \mathbf{H}_h \rrbracket - \rho^+ c_s^+ [\mathbf{w}_h]))) \\
 &\quad + 4 \rho^- c_s^- ((\mathbf{E}_h^- - \text{tr}(\mathbf{E}_h^-) \mathbf{I}) \mathbf{n}^-) \cdot \mathbf{w}_h^-, \tag{45}
 \end{aligned}$$

where $(\mathbf{v}_h, \mathbf{E}_h)$ is the solution of the state equation (41) and $(\mathbf{w}_h, \mathbf{H}_h)$ is the solution of the adjoint equation (43). Note that since we allow for discontinuous wave speeds c_p and c_s (and perturbations \tilde{c}_p and \tilde{c}_s), the boundary contributions to the gradients, i.e., the last terms in (44a) and (45) are written as sums of integrals over individual element boundaries, i.e., each boundary face appears twice in the overall sum. This differs from the previous examples, where we assumed continuous parameters and thus combined contributions from adjacent elements to shared faces f .

Remark 7 The expressions for the c_p -gradient (44) reduce to the result found for the acoustic equation (27) and (29) for continuous parameter fields ρ, c_p, c_s and continuous parameter perturbations \tilde{c}_p . To verify this, one adds contributions from adjacent elements to common boundaries, and the terms in (44b) combine or cancel.

Remark 8 Above, we have derived expressions for the derivatives with respect to the primary and secondary wave speeds. If, instead of c_p and c_s , derivatives with respect to an alternative pair of parameters in the stress tensor—such as the Lamé parameters, or Poisson’s ratio and Young’s modulus—are derived, the adjoint equations remain unchanged, but the expressions for the derivatives change according to the chain rule.

4 Numerical Verification for Coupled Elastic-Acoustic Wave Propagation

Here, we numerically verify the expressions for the discrete gradients with respect to the wave speeds for the elastic-acoustic wave problem derived in Sect. 3.4. For this purpose, we compare directional finite differences with directional gradients based on the discrete gradient. To emphasize the correctness of the discrete gradient, we use coarse meshes in these comparisons, which are not able to fully resolve the wave fields. As test problem, we use the Snell law example from Sect. 6.2 in [40] with the material parameters and the wave incident angle specified there. For our tests, we use the simple distributed objective function

$$\mathcal{J}(c_p, c_s) := \int_0^T \int_{\Omega} \mathbf{v}_h \cdot \mathbf{v}_h \, dx \, dt.$$

The discretization of the wave equation follows [40], i.e., we use spectral elements based on Gauss-Lobatto-Lagrange (GLL) points on hexahedral meshes. The use of GLL quadrature results in underintegration even if the elements are images of the reference element under an affine transformation. In Fig. 2, we summarize results for the directional derivatives in the direction $\tilde{c}_p := \sin(\pi x) \cos(\pi y) \cos(\pi z)$; we compare the finite difference directional derivatives

$$d_{\epsilon}^{\text{fd}} := \frac{\mathcal{J}(c_p + \epsilon \tilde{c}_p) - \mathcal{J}(c_p)}{\epsilon} \tag{46}$$

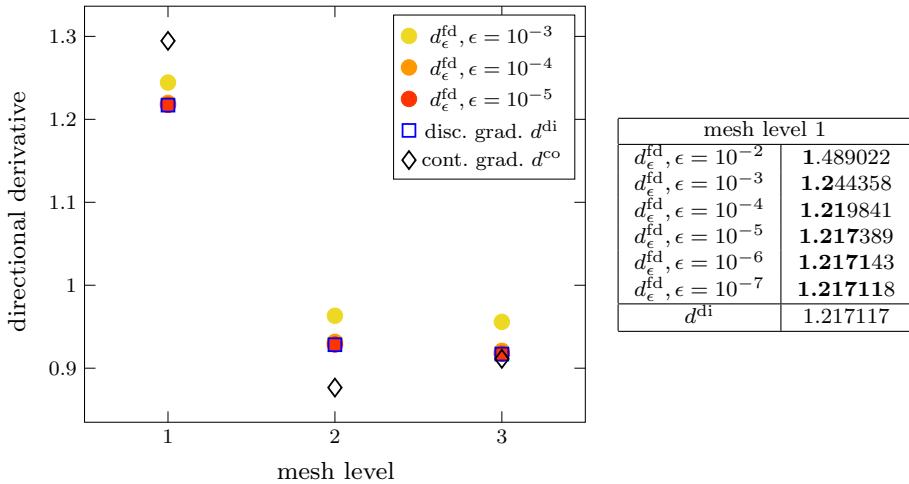


Fig. 2 Directional derivatives computed using one-sided finite differences (46), and the discrete and the continuous gradients (47). Left: Results on mesh levels 1, 2 and 3 corresponding to meshes with 16, 128 and 1,024 finite elements with polynomial order $N = 4$. The finite difference directional derivatives d_ϵ^{fd} converge to the discrete gradient d^{di} as ϵ is reduced. Note that as the mesh level is increased, the continuous gradient d^{co} converges to d^{di} . Right: Convergence of finite difference directional derivative on the coarsest mesh (level 1). Digits for which the finite difference gradient coincides with the discrete gradient are shown in bold

with the directional derivatives d^{di} and d^{co} defined by

$$d^{\text{di}} := \mathcal{J}_{c_p}(c_p, c_s)(\tilde{c}_p), \quad d^{\text{co}} := \mathcal{J}_{c_p}^{\text{co}}(c_p, c_s)(\tilde{c}_p), \tag{47}$$

where $\mathcal{J}_{c_p}(c_p, c_s)$ denotes the discrete gradient (44), and $\mathcal{J}_{c_p}^{\text{co}}(c_p, c_s)$ denotes the gradient obtained when neglecting the jump term in the boundary contributions g_p in (44b). These jump terms are likely to be neglected if the continuous gradient expressions are discretized instead of following a fully discrete approach. The resulting error is of the order of the discretization error and thus vanishes as the discrete solutions converge. However, this error can be significant on coarse meshes, on which the wave solution is not well resolved.

Next, we study the accuracy of the discrete gradient for pointwise perturbations to the wave speed. Since the same discontinuous basis functions as for the wave equation are also used for the local wave speeds, a point perturbation in c_p^- or c_s^- at an element boundary face results in a globally discontinuous perturbation direction \tilde{c}_p and \tilde{c}_s . In Table 1, we present the discrete directional gradient d^{di} with finite difference directional gradients d_ϵ^{fd} for unit vector perturbations of both wave speeds. Compared to in the table in Fig. 2, where the directional derivatives for smooth perturbations are reported, pointwise perturbations of the wave speeds c_p or c_s result in smaller changes in the cost functional, and numerical roundoff influences the accuracy of finite difference directional derivatives. As a consequence, fewer digits coincide between the finite difference directional derivatives and the discrete gradients.

5 Conclusions

Our study yields that the discretely exact adjoint PDE of a dG-discretized linear hyperbolic equation is a proper dG discretization of the continuous adjoint equation, provided an upwind flux is used. Thus, the adjoint PDE converges at the same rate as the state equation. When

Table 1 Comparison of pointwise material gradients for Snell problem from [40, Sect. 6.2]

Mesh level #tsteps	(x, y, z)	Pert. field	d^{di}	d_{ϵ}^{fd}		
				$\epsilon = 10^{-3}$	$\epsilon = 10^{-4}$	$\epsilon = 10^{-5}$
1/101	(0, 0, 0)	c_p	1.8590e-4	1.8549e-4	1.8581e-4	1.8560e-4
2/202	(0, 0, 0)	c_p	2.2102e-5	2.2094e-5	2.2007e-5	2.1504e-5
1/101	(0, 0, 1)	c_s	1.1472e-5	1.1453e-5	1.1372e-5	1.0942e-5
1/101	(-0.5, -0.5, 0.5)	c_s	2.8886e-3	2.8802e-3	2.8877e-3	2.8870e-3

The derivatives d_{ϵ}^{fd} and d^{di} with respect to the local wave speed (either c_p or c_s) for points with coordinates (x, y, z) are reported. We use the final time $T = 1$ and spectral elements of polynomial order $N = 6$ in space. The meshes for level 1 and 2 consist of 16 and 128 finite elements, respectively. Digits where the finite difference approximation coincides with the discrete gradient are shown in bold

integration by parts is avoided to eliminate quadrature errors, a weak dG discretization of the state PDE leads to a strong dG discretization of the adjoint PDE, and vice versa. The expressions for the discretely exact gradient can contain contributions at element faces and, hence, differ from a straightforward discretization of the continuous gradient expression. These element face contributions are at the order of the discretization error and are thus more significant for under resolved state and adjoint solutions. We believe that these observations are relevant for inverse problems and optimal control problems governed by hyperbolic PDEs discretized by the discontinuous Galerkin method.

Acknowledgments We would like to thank Jeremy Kozdon and Gregor Gassner for fruitful discussions and helpful comments, and Carsten Burstedde for his help with the implementation of the numerical example presented in Sect. 4. Support for this work was provided through the U.S. National Science Foundation (NSF) grant CMMI-1028889, the Air Force Office of Scientific Research's Computational Mathematics program under the grant FA9550-12-1-0484, and through the Mathematical Multifaceted Integrated Capability Centers (MMICCs) effort within the Applied Mathematics activity of the U.S. Department of Energy's Advanced Scientific Computing Research program, under Award Number DE-SC0009286. The views expressed in this document are those of the authors and do not reflect the official policy or position of the Department of Defense or the U.S. Government.

References

- Alexe, M., Sandu, A.: Space-time adaptive solution of inverse problems with the discrete adjoint method. *J. Comput. Phys.* **270**, 21–39 (2014). doi:[10.1016/j.jcp.2014.03.042](https://doi.org/10.1016/j.jcp.2014.03.042)
- Becker, R., Meindner, D., Vexler, B.: Efficient numerical solution of parabolic optimization problems by finite element methods. *Optim. Methods Softw.* **22**, 813–833 (2007). doi:[10.1080/10556780701228532](https://doi.org/10.1080/10556780701228532)
- Borzi, A., Schulz, V.: *Computational Optimization of Systems Governed by Partial Differential Equations*. SIAM, Philadelphia (2012). doi:[10.1137/1.9781611972054](https://doi.org/10.1137/1.9781611972054)
- Braack, M.: Optimal control in fluid mechanics by finite elements with symmetric stabilization. *SIAM J. Control Optim.* **48**, 672–687 (2009). doi:[10.1137/060653494](https://doi.org/10.1137/060653494)
- Bui-Thanh, T., Burstedde, C., Ghattas, O., Martin, J., Stadler, G., Wilcox, L.C.: Extreme-scale UQ for Bayesian inverse problems governed by PDEs. In: *SC12 Proceedings of the International Conference for High Performance Computing, Networking, Storage and Analysis* (2012). doi:[10.1109/SC.2012.56](https://doi.org/10.1109/SC.2012.56)
- Bui-Thanh, T., Ghattas, O., Martin, J., Stadler, G.: A computational framework for infinite-dimensional Bayesian inverse problems part I: the linearized case, with application to global seismic inversion. *SIAM J. Sci. Comput.* **35**, A2494–A2523 (2013). doi:[10.1137/12089586X](https://doi.org/10.1137/12089586X)
- Collis, S.S., Heinkenschloss, M.: Analysis of the streamline upwind/Petrov Galerkin method applied to the solution of optimal control problems. Technical Report TR02-01, Department of Computational

- and Applied Mathematics, Rice University, Houston, TX 77005–1892 (2002). <http://www.caam.rice.edu/~heinken>
8. Collis, S.S., Ober, C.C., van Bloemen Waanders, B.G.: Unstructured discontinuous Galerkin for seismic inversion. In: Conference Paper, SEG International Exposition and 80th Annual Meeting (2010)
 9. Epanomeritakis, I., Akçelik, V., Ghattas, O., Bielak, J.: A Newton-CG method for large-scale three-dimensional elastic full-waveform seismic inversion. *Inverse Probl.* **24** (2008), 034015 (26pp). doi:[10.1088/0266-5611/24/3/034015](https://doi.org/10.1088/0266-5611/24/3/034015)
 10. Feng, K.-A., Teng, C.-H., Chen, M.-H.: A pseudospectral penalty scheme for 2D isotropic elastic wave computations. *J. Sci. Comput.* **33**, 313–348 (2007). doi:[10.1007/s10915-007-9154-8](https://doi.org/10.1007/s10915-007-9154-8)
 11. Fichtner, A.: *Full Seismic Waveform Modelling and Inversion*. Springer, Berlin (2011)
 12. Giles, M., Pierce, N.: Adjoint equations in CFD: duality, boundary conditions and solution behaviour. American Institute of Aeronautics and Astronautics (1997). doi:[10.2514/6.1997-1850](https://doi.org/10.2514/6.1997-1850)
 13. Giles, M., Ulbrich, S.: Convergence of linearized and adjoint approximations for discontinuous solutions of conservation laws. Part 1: linearized approximations and linearized output functionals. *SIAM J. Numer. Anal.* **48**, 882–904 (2010). doi:[10.1137/080727464](https://doi.org/10.1137/080727464)
 14. Giles, M., Ulbrich, S.: Convergence of linearized and adjoint approximations for discontinuous solutions of conservation laws. Part 2: adjoint approximations and extensions. *SIAM J. Numer. Anal.* **48**, 905–921 (2010). doi:[10.1137/09078078X](https://doi.org/10.1137/09078078X)
 15. Griewank, A., Walther, A.: Algorithm 799: revolve: an implementation of checkpointing for the reverse or adjoint mode of computational differentiation. *ACM Trans. Math. Softw.* **26**, 19–45 (2000). doi:[10.1145/347837.347846](https://doi.org/10.1145/347837.347846)
 16. Griewank, A., Walther, A.: *Evaluating Derivatives: Principles and Techniques of Algorithmic Differentiation*, 2nd edn. SIAM, Philadelphia (2008). doi:[10.1137/1.9780898717761](https://doi.org/10.1137/1.9780898717761)
 17. Gunzburger, M.D.: *Perspectives in Flow Control and Optimization*. SIAM, Philadelphia (2003). doi:[10.1137/1.9780898718720](https://doi.org/10.1137/1.9780898718720)
 18. Gustafsson, B., Kreiss, H.-O., Olinger, J.: *Time Dependent Problems and Difference Methods*. Wiley, New York (1995)
 19. Hager, W.W.: Runge-Kutta methods in optimal control and the transformed adjoint system. *Numer. Math.* **87**, 247–282 (2000). doi:[10.1007/s002110000178](https://doi.org/10.1007/s002110000178)
 20. Harriman, K., Gavaghan, D., Süli, E.: The importance of adjoint consistency in the approximation of linear functionals using the discontinuous Galerkin finite element method. Technical Report NA04/18, Oxford University Computing Laboratory (2004)
 21. Hartmann, R.: Adjoint consistency analysis of discontinuous Galerkin discretizations. *SIAM J. Numer. Anal.* **45**, 2671–2696 (2007). doi:[10.1137/060665117](https://doi.org/10.1137/060665117)
 22. Hesthaven, J.S., Warburton, T.: Nodal high-order methods on unstructured grids. I. Time-domain solution of Maxwell's equations. *J. Comput. Phys.* **181**, 186–221 (2002). doi:[10.1006/jcph.2002.7118](https://doi.org/10.1006/jcph.2002.7118)
 23. Hesthaven, J.S., Warburton, T.: *Nodal Discontinuous Galerkin Methods: Algorithms, Analysis, and Applications*, vol. 54 of Texts in Applied Mathematics. Springer, Berlin (2008)
 24. Hinze, M., Pinnau, R., Ulbrich, M., Ulbrich, S.: *Optimization with PDE Constraints*. Springer, Berlin (2009)
 25. Kopriva, D.A.: *Implementing Spectral Methods for Partial Differential Equations*. Springer, Berlin (2009)
 26. Kopriva, D.A., Gassner, G.: On the quadrature and weak form choices in collocation type discontinuous Galerkin spectral element methods. *J. Sci. Comput.* **44**, 136–155 (2010). doi:[10.1007/s10915-010-9372-3](https://doi.org/10.1007/s10915-010-9372-3)
 27. Lagnese, J.E.: Exact boundary controllability of Maxwell's equations in a general region. *SIAM J. Control Optim.* **27**, 374–388 (1989). doi:[10.1137/0327019](https://doi.org/10.1137/0327019)
 28. Lekić, V., Romanowicz, B.: Inferring upper-mantle structure by full waveform tomography with the spectral element method. *Geophys. J. Int.* **185**, 799–831 (2011). doi:[10.1111/j.1365-246X.2011.04969.x](https://doi.org/10.1111/j.1365-246X.2011.04969.x)
 29. Leykekhman, D.: Investigation of commutative properties of discontinuous Galerkin methods in PDE constrained optimal control problems. *J. Sci. Comput.* **53**, 483–511 (2012). doi:[10.1007/s10915-012-9582-y](https://doi.org/10.1007/s10915-012-9582-y)
 30. Lions, J.-L.: *Control of Distributed Singular Systems*. Gauthier-Villars, Paris (1985)
 31. Mohammadian, A.H., Shankar, V., Hall, W.F.: Computational of electromagnetic scattering and radiation using a time-domain finite-volume discretization procedure. *Comput. Phys. Commun.* **68**, 175–196 (1991). doi:[10.1016/0010-4655\(91\)90199-U](https://doi.org/10.1016/0010-4655(91)90199-U)
 32. Nicaise, S.: Exact boundary controllability of Maxwell's equations in heterogeneous media and an application to an inverse source problem. *SIAM J. Control Optim.* **38**, 1145–1170 (2000). doi:[10.1137/S0363012998344373](https://doi.org/10.1137/S0363012998344373)
 33. Oliver, T.A., Darmofal, D.L.: Analysis of dual consistency for discontinuous Galerkin discretizations of source terms. *SIAM J. Numer. Anal.* **47**, 3507–3525 (2009). doi:[10.1137/080721467](https://doi.org/10.1137/080721467)
 34. Peter, D., Komatitsch, D., Luo, Y., Martin, R., Le Goff, N., Casarotti, E., Le Locher, P., Magnoni, F., Liu, Q., Blitz, C., Nisson-Meyer, T., Basini, P., Tromp, J.: Forward and adjoint simulations of seismic wave

- propagation on fully unstructured hexahedral meshes. *Geophys. J. Int.* **186**, 721–739 (2011). doi:[10.1111/j.1365-246X.2011.05044.x](https://doi.org/10.1111/j.1365-246X.2011.05044.x)
35. Schütz, J., May, G.: An adjoint consistency analysis for a class of hybrid mixed methods. *IMA J. Numer. Anal.* **34**(3), 863–878 (2013). doi:[10.1093/imanum/drt036](https://doi.org/10.1093/imanum/drt036)
 36. Teng, C.-H., Lin, B.-Y., Chang, H.-C., Hsu, H.-C., Lin, C.-N., Feng, K.-A.: A legendre pseudospectral penalty scheme for solving time-domain Maxwell's equations. *J. Sci. Comput.* **36**, 351–390 (2008). doi:[10.1007/s10915-008-9194-8](https://doi.org/10.1007/s10915-008-9194-8)
 37. Tröltzsch, F.: *Optimal Control of Partial Differential Equations: Theory, Methods and Applications*, vol. 112 of Graduate Studies in Mathematics. American Mathematical Society (2010)
 38. Utke, J., Hascoët, L., Heimbach, P., Hill, C., Hovland, P., Naumann, U.: Toward adjoinable MPI. In: *IEEE International Symposium on Parallel & Distributed Processing*, 2009. IPDPS 2009, pp. 1–8 (2009). doi:[10.1109/IPDPS.2009.5161165](https://doi.org/10.1109/IPDPS.2009.5161165)
 39. Walther, A.: Automatic differentiation of explicit Runge–Kutta methods for optimal control. *Comput. Optim. Appl.* **36**, 83–108 (2007). doi:[10.1007/s10589-006-0397-3](https://doi.org/10.1007/s10589-006-0397-3)
 40. Wilcox, L.C., Stadler, G., Burstedde, C., Ghattas, O.: A high-order discontinuous Galerkin method for wave propagation through coupled elastic-acoustic media. *J. Comput. Phys.* **229**, 9373–9396 (2010). doi:[10.1016/j.jcp.2010.09.008](https://doi.org/10.1016/j.jcp.2010.09.008)
 41. Yousept, I.: Optimal control of Maxwell's equations with regularized state constraints. *Comput. Optim. Appl.* **52**, 559–581 (2012). doi:[10.1007/s10589-011-9422-2](https://doi.org/10.1007/s10589-011-9422-2)